(12) INTERNATIONAL APPLICATION PUBLISHED UNDER THE PATENT COOPERATION TREATY (PCT)

(19) World Intellectual Property Organization
International Bureau

(43) International Publication Date
8 July 2004 (08.07.2004)

PCT

(10) International Publication Number
WO 2004/057391 A1

(51) International Patent Classification[7]: G02B 6/16, 6/20, C03B 37/012

(21) International Application Number: PCT/GB2003/005591

(22) International Filing Date: 22 December 2003 (22.12.2003)

(25) Filing Language: English

(26) Publication Language: English

(30) Priority Data:

0229826.3	20 December 2002 (20.12.2002)	GB
0302632.5	5 February 2003 (05.02.2003)	GB
0306606.5	21 March 2003 (21.03.2003)	GB
0306593.5	21 March 2003 (21.03.2003)	GB
0314485.4	20 June 2003 (20.06.2003)	GB

(71) Applicant *(for all designated States except US)*: **BLAZEPHOTONICS LIMITED** [GB/GB]; Finance Office, University of Bath, The Avenue,Claverton Down, Bath BA2 7AY (GB).

(72) Inventors; and

(75) Inventors/Applicants *(for US only)*: **WILLIAMS, David, Philip** [GB/GB]; Flat 7, 27 Marlborough Buildings, Bath BA1 2LY (GB). **BIRKS, Timothy, Adam** [GB/GB]; 14 Horsecombe Brow, Combe Down, Bath BA2 5QY (GB). **RUSSELL, Philip, St. John** [GB/GB]; Shepherds Mead, Southstoke, Bath BA2 7EB (GB). **ROBERTS, Peter, John** [GB/GB]; 11 Gladstone Road, Bath BA2 5HJ (GB). **SABERT, Hendrik** [DE/GB]; Flat 2, 19 Royal Crescent, Bath BA1 2LT (GB).

(74) Agents: **CRITTEN, Matthew, Peter** et al.; Abel & Imray, 20 Red Lion Street, London WC1R 4PQ (GB).

(81) Designated States *(national)*: AE, AG, AL, AM, AT, AU, AZ, BA, BB, BG, BR, BW, BY, BZ, CA, CH, CN, CO, CR,

[Continued on next page]

(54) Title: OPTICAL WAVEGUIDE

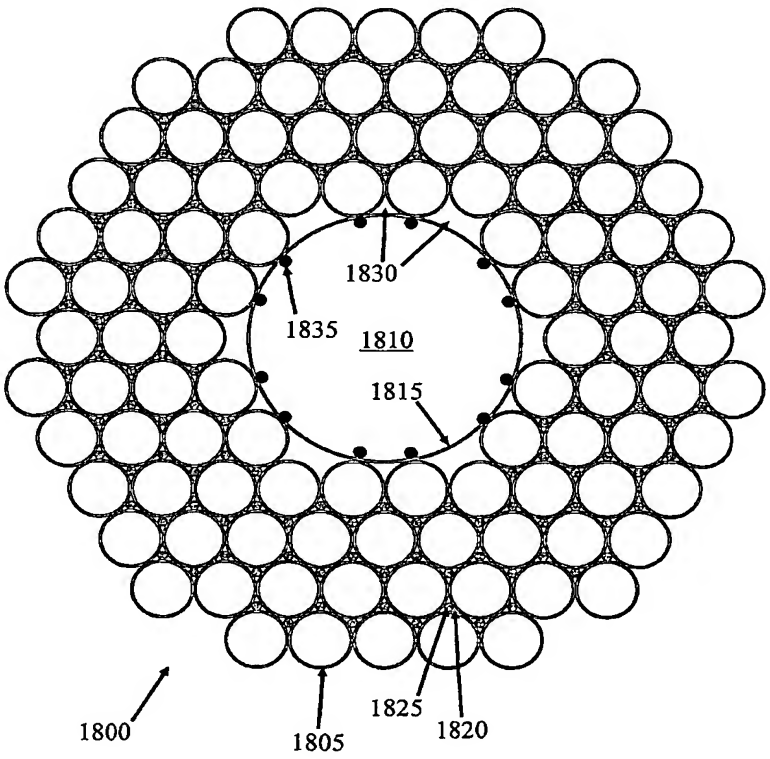

(57) Abstract: The present invention is in the field of optical fibres. In particular, the present inventors describe hollow core optical fibres, for example hollow core photonic band-gap optical fibres. The present inventors describe examples of such fibres that guide light by virtue of a true photonic band-gap in a hollow core region having a boundary at the interface between the hollow core and a photonic band-gap cladding. In some examples, the boundary is tuned by addition of solid material during formation of a respective fibre preform (1800) to improve the performance of the resulting fibre, for example by mitigating deleterious effects such as mode coupling of light from core-guided modes to so-called boundary or 'surface' modes.

WO 2004/057391 A1

CU, CZ, DE, DK, DM, DZ, EC, EE, EG, ES, FI, GB, GD, GE, GH, GM, HR, HU, ID, IL, IN, IS, JP, KE, KG, KP, KR, KZ, LC, LK, LR, LS, LT, LU, LV, MA, MD, MG, MK, MN, MW, MX, MZ, NI, NO, NZ, OM, PG, PH, PL, PT, RO, RU, SC, SD, SE, SG, SK, SL, SY, TJ, TM, TN, TR, TT, TZ, UA, UG, US, UZ, VC, VN, YU, ZA, ZM, ZW.

(84) **Designated States** *(regional)*: ARIPO patent (BW, GH, GM, KE, LS, MW, MZ, SD, SL, SZ, TZ, UG, ZM, ZW), Eurasian patent (AM, AZ, BY, KG, KZ, MD, RU, TJ, TM), European patent (AT, BE, BG, CH, CY, CZ, DE, DK, EE, ES, FI, FR, GB, GR, HU, IE, IT, LU, MC, NL, PT, RO, SE, SI, SK, TR), OAPI patent (BF, BJ, CF, CG, CI, CM, GA, GN, GQ, GW, ML, MR, NE, SN, TD, TG).

Published:

— *with international search report*

For two-letter codes and other abbreviations, refer to the "Guidance Notes on Codes and Abbreviations" appearing at the beginning of each regular issue of the PCT Gazette.

Optical Waveguide

Technical Field

The present invention is in the field of optical waveguides and relates in particular to optical waveguides that guide light by virtue of a photonic bandgap.

Background Art

Optical fibre waveguides, which are able to guide light by virtue of a so-called photonic bandgap (PBG), were first proposed in 1995.

In, for example, "Full 2-D photonic bandgaps in silica/air structures", Birks et al., Electronics Letters, 26 October 1995, Vol. 31, No. 22, pp.1941-1942, it was proposed that a PBG may be created in an optical fibre by providing a dielectric cladding structure, which has a refractive index that varies periodically between high and low index regions, and a core defect in the cladding structure in the form of a hollow core. In the proposed cladding structure, periodicity was provided by an array of air holes that extended through a silica glass matrix material to provide a PBG structure through which certain wavelengths and propagation constants of light could not pass. It was proposed that light coupled into the hollow core defect would be unable to escape into the cladding due to the PBG and, thus, the light would remain localised in the core defect.

It was appreciated that light travelling through a hollow core defect, for example filled with air or even under vacuum, would suffer significantly less from undesirable effects, such as non-linearity and loss, compared with light travelling through a solid silica or doped silica fibre core. As such, it was appreciated that a PBG fibre may find application as a transmission fibre to transmit light over extremely long distances, for example across the Atlantic Ocean, without undergoing signal regeneration or as a high optical power delivery waveguide. In contrast, for standard index-guiding, single mode optical fibre, signal regeneration is typically required approximately every 80 kilometres.

The first hollow core PBG fibres that were attempted by the inventors had a periodic cladding structure formed by a triangular array of circular air holes embedded in a solid silica matrix and surrounding a central air core defect. Such fibres were formed by stacking circular or hexagonal capillary tubes, incorporating a core defect into the cladding by omitting a central capillary of the stack, and then heating and drawing the stack, in a one or two step process, to form a fibre having the required structure. The first fibres made by this process

had a core defect formed by the omission of a single capillary from the centre of the cladding structure.

US patent application US6404966 describes what is stated therein to be a PBG fibre having a hollow core region, which has an area of several times the optical wavelength, and a PBG cladding having a pitch equal to half the optical wavelength. The suggested advantage of the fibre is that it exhibits single mode behaviour.

International patent application PCT/GB00/01249 (The Secretary of State for Defence, UK), filed on 21 March 2000, proposed the first PBG fibre to have a so-called seven-cell core defect, surrounded by a cladding comprising a triangular array of air holes embedded in an all-silica matrix. The core defect was formed by omitting an inner capillary and, in addition, the six capillaries surrounding the inner capillary. This fibre structure appeared to guide one or two modes in the core defect, in contrast to the previous, single-cell core defect fibre, which appeared not to support any guided modes in the core defect.

According to PCT/GB00/01249, it appeared that the single-cell core defect fibre, by analogy to the density-of-states calculations in solid-state physics, would only support approximately 0.23 modes. That is, it was not surprising that the single-cell core defect fibre appeared to support no guided modes in its core defect. In contrast, based on the seven-fold increase in core defect area (increasing the core defect radius by a factor of $\sqrt{7}$), the seven-cell core defect fibre was predicted to support approximately 1.61 spatial modes in the core defect. This prediction was consistent with the finding that the seven-cell core defect fibre did indeed appear to support at least one guided mode in its core defect.

A preferred fibre in PCT/GB00/01249 was described as having a core defect diameter of around 15μm and an air-filling fraction (AFF) – that is, the proportion by volume of air in the cladding - of greater than 15% and, preferably, greater than 30%. Herein, AFF (or any equivalent measure for air or vacuum or other materials) is intended to mean the fraction by volume of air in a microstructured, or holey, portion of the cladding, which is representative of a substantially perfect and unbounded cladding. That is, imperfect regions of the cladding, for example near to or abutting a core defect and at an outer periphery of a microstructured region, would not be used in calculating the AFF. Likewise, a calculation of AFF does not take into account over-cladding or jacketing layers, which may surround the microstructured region.

In "Analysis of air-guiding photonic bandgap fibres", Optics Letters, Vol. 25, No. 2, January 15, 2000, Broeng et al. provided a theoretical analysis of PBG fibres. For a fibre with

a seven-cell core defect and a cladding comprising a triangular array of near-circular holes, providing an AFF of around 70%, the structure was shown to support one or two air guided modes in the core defect. This was in line with the finding in PCT/GB00/01249.

In the chapter entitled "Photonic Crystal Fibers: Effective Index and Band-Gap Guidance" from the book "Photonic Crystal and Light Localization in the 21st Century", C.M. Soukoulis (ed.), ©2001 Kluwer Academic Publishers, the authors presented further analysis of PBG fibres based primarily on a seven-cell core defect fibre. The optical fibre was fabricated by stacking and drawing hexagonal silica capillary tubes. The authors suggested that a core defect must be large enough to support at least one guided mode but that, as in conventional fibres, increasing the core defect size would lead to the appearance of higher order modes. This statement appears to contradict the position presented in the aforementioned US6404966, which prescribes a large core region and single mode behaviour. The authors of the chapter also went on to suggest that there are many parameters that can have a considerable influence on the performance of bandgap fibres: choice of cladding lattice, lattice spacing, index filling fraction, choice of materials, size and shape of core defect, and structural uniformity (both in-plane and along the axis of propagation).

WO 02/075392 (Corning, Inc.) identifies a general relationship in PBG fibres between the number of so–called surface modes that exist at the boundary between the cladding and core defect of a PBG fibre and the ratio of the radial size of the core defect and a pitch of the cladding structure, where pitch is the centre to centre spacing of nearest neighbour holes in the triangular array of the exemplified cladding structure. It is suggested that when the core defect boundary, together with the photonic bandgap crystal pitch, are such that surface modes are excited or supported, a large fraction of the "light power" propagated along the fibre is essentially not located in the core defect. Accordingly, while surface states exist, the suggestion was that the distribution of light power is not effective to realise the benefits associated with the low refractive index core defect of a PBG crystal optical waveguide. The mode energy fraction in the core defect of the PBG fibre was shown to vary with increasing ratio of core defect size to pitch. In other words, it was suggested that the way to increase mode energy fraction in the core defect is by decreasing the number of surface modes, in turn, by selecting an appropriate ratio of the radial size of the core defect and a pitch of the cladding structure. In particular, WO 02/075392 states that, for a circular core structure, a ratio of core radius to pitch of around 1.07 to 1.08 provides a high mode power fraction of not

less than 0.9 and is single mode. Other structures are considered, for example in Figure 7, wherein the core defect covers an area equivalent to 16 cladding holes.

In a Post-deadline paper presented at ECOC 2002, "Low Loss (13dB) Air core defect Photonic Bandgap Fibre", N. Venkataraman et al. reported a PBG fibre having a seven-cell core defect that exhibited loss as low as 13dB/km at 1500nm over a fibre length of one hundred metres. The structure of this fibre closely matches the structure considered in the book chapter referenced above. The authors attribute the relatively small loss of the fibre as being due to the high degree of structural uniformity along the length of the fibre.

PBG fibre structures are typically fabricated by first forming a pre-form and then heating and drawing an optical fibre from that pre-form in a fibre-drawing tower. It is known either to form a pre-form by stacking capillaries and fusing the capillaries into the appropriate configuration of pre-form, or to use extrusion.

For example, in PCT/GB00/01249, identified above, a seven-cell core defect pre-form structure was formed by omitting from a stack of capillaries an inner capillary and, in addition, the six capillaries surrounding the inner capillary. The capillaries around the core defect boundary in the stack were supported during formation of the pre-form by inserting truncated capillaries, which did not meet in the middle of the stack, at both ends of the capillary stack. The stack was then heated in order to fuse the capillaries together into a pre-form suitable for drawing into an optical fibre. Clearly, only the fibre drawn from the middle section of the stack, with the missing inner seven capillaries, was suitable for use as a hollow core defect fibre.

US patent application number US 6,444,133 (Corning, Inc.), describes a technique of forming a PBG fibre pre-form comprising a stack of hexagonal capillaries in which the inner capillary is missing, thus forming a core defect of the eventual PBG fibre structure that has flat inner surfaces. In contrast, the holes in the capillaries are circular. US 6,444,133 proposes that, by etching the entire pre-form, the flat surfaces of the core defect dissolve away more quickly than the curved surfaces of the outer capillaries. The effect of etching is that the edges of the capillaries that are next to the void fully dissolve, while the remaining capillaries simply experience an increase in hole-diameter. Overall, the resulting pre-form has a greater fraction of air in the cladding structure and a core defect that is closer to a seven-cell core defect than a single cell core defect.

PCT patent application number WO 02/084347 (Corning, Inc.) describes a method of making a pre-form comprising a stack of hexagonal capillaries of which the inner capillaries

are preferentially etched by exposure to an etching agent. Each capillary has a hexagonal outer boundary and a circular inner boundary, as illustrated in the diagram in Figure 11 herein. The result of the etching step is that the centres of the edges of the hexagonal capillaries around the central region dissolve more quickly than the corners, thereby causing formation of a core defect. In some embodiments, the circular holes are offset in the inner hexagonal capillaries of the stack so that each capillary has a wall that is thinner than its opposite wall. These capillaries are arranged in the stack so that their thinner walls point towards the centre of the structure. An etching step, in effect, preferentially etches the thinner walls first, thereby forming a seven-cell core defect.

Disclosure of the Invention

In arriving at the present invention, the inventors have demonstrated that, while the size of a core defect is significant in determining certain characteristics of a PBG waveguide, the form of a boundary at the interface between core and cladding also plays a significant role in determining certain characteristics of the waveguide. As will be described in detail hereafter, the inventors have determined that, for given PBG core and cladding structures, variations in only the form of the boundary can cause significant changes in the characteristics of a respective waveguide.

According to a first aspect, the present invention provides an elongate waveguide for guiding light comprising:

a core, comprising an elongate region of relatively low refractive index;

a microstructured region around the core comprising elongate regions of relatively low refractive index interspersed with elongate regions of relatively high refractive index; and

a boundary at the interface between the core and the microstructured region, the boundary comprising, in the transverse cross-section, a region of relatively high refractive index, which is connected to the microstructured region at a plurality of nodes, characterised by at least one relatively enlarged region around the boundary (and excluding a boundary having twelve nodes and six enlarged regions substantially at a mid-point between six pairs of relatively more-widely-spaced apart neighbouring nodes).

As used herein, the term "relatively enlarged region" may have various different meanings depending upon the particular form of the boundary. For example, a relatively enlarged region may mean a bead-like formation or a locally thicker region along a relatively thinner boundary. A bead-like formation may be substantially oval in shape and have its

major axis oriented radially or azimuthally with respect to the centre of the waveguide structure. Alternatively, a relatively enlarged region may mean a nodule, outcrop, lump or projection, on either an inner or outer periphery of the boundary. Alternatively, a relatively enlarged region may mean a relatively thicker region around the boundary. Embodiments of the present invention apply one or more of these kinds of features, as will be described hereinafter.

The boundary region is a continuous shell of relatively high refractive index in that it does not comprise regions of relatively low refractive index: all relatively-high-index regions in the boundary are connected to each other only by relatively-high-index regions. The core is taken to be contiguous with the boundary region. The core thus comprises all connected regions of relatively low refractive index that are surrounded by the boundary region. The boundary region may be not smooth: it may for example be corrugated, with indented regions (for example, formed by omitting every other vein from an innermost polygon of the cladding, such as what would, if all veins were present, be an hexagon defining an hexagonal core), or it may have one two or more struts that project towards the centre of the core (which struts may be of uniform thickness or may have nodules at some point along their length, for example at their ends). Thus, the core need not be of a regular cross section but may, for example, have projections and indentations defined by the boundary region.

Thus the boundary region may be corrugated with 2, 3, 4, 5, 6, 7, 8, 9, 10 or more recesses or indentations, which may be arranged at regular intervals around the centre of the core.

The present invention excludes a prior art PBG fibre structure of the kind described in the aforementioned book chapter. This particular kind of structure, which is illustrated in Figure 1 in the accompanying drawings, and which is attributed with having attained the aforementioned 13dB/km loss figure, has been discussed in numerous papers and articles since 2001. The structure itself, however, has not changed, it having bead-like formations 165 along consecutive longer sides 140 of the boundary 145 around the core region 110. The beadlike formations are merely an artefact and natural consequence of using hexagonal cross section capillaries, or the process used to make the fibre, as described in further detail hereinafter with reference to Figure 1. Even relatively recently, this same PBG fibre structure has been considered in detail in "Surface modes and loss in air-core photonic band-gap fibers", Allan et al., Photonic Crystal Materials and Devices, Proceedings of SPIE, Volume 5000, 28-30 January 2003. In that paper, the authors provided a study of the fibre structure

and attributed a certain amount of loss in the fibre as being due to mode coupling of light from core modes to so-called 'surface modes', which exist around the core boundary. The present inventors have discovered that, according to embodiments of the present invention, it is possible to use similar bead-like formations, among many other configurations of core boundary, to tune the modal properties of a given PBG fibre. In some cases, it is believed that embodiment of the present invention may be used to mitigate the deleterious effects of the aforementioned mode coupling by de-tuning the surface modes, either by removing them or shifting them further from the core modes.

Considering, for example, an air-core and silica PBG fibre, the inventors have determined that the geometry of the region of the boundary between the air core and the photonic bandgap cladding structure has profound effects on the modal properties of the fibre. In particular, the inventors have appreciated that the number of guiding modes within the band gap, the relative position of those guided modes in the modal spectrum, the fraction of the light power of the guided modes confined within the air core and the field intensity of these modes at the air-silica interfaces all vary sensitively with the geometry within the region. In particular, the inventors have shown that by tailoring the geometry, the properties of an LP_{01}-like mode (when present), which possesses an approximately Gaussian intensity profile towards the centre of the core, can be tailored so that up to and even over 99% of the light is confined within air, and predominantly in the core. This implies that loss due to Rayleigh scattering in the silica may be suppressed by up to two orders of magnitude and that nonlinearity may be substantially reduced compared with standard index guiding single mode fibre. Also, the inventors have demonstrated that the core boundary geometry can be designed to reduce the field intensity of this mode strongly in the vicinity of the air-silica interfaces. This has the effect of reducing both the small scale interface roughness scattering, which is discussed in detail hereafter, and the mode coupling due to longer range fibre variations.

According to embodiments of the invention that are described hereinafter, there are plural enlarged regions around the boundary. The or at least one enlarged region may be positioned between neighbouring nodes.

There may in some embodiments be six enlarged regions around the boundary, or there may be more than six enlarged regions around the boundary. For example, there may be twelve or more enlarged regions around the boundary.

In some embodiments, the core boundary may comprise eighteen nodes. There may be enlarged regions between six or more pairs of neighbouring nodes. For example, the boundary may have enlarged regions between twelve pairs of neighbouring nodes.

In some examples, there is only one enlarged region between any pair of neighbouring nodes. In other examples, there are plural enlarged regions between at least one pair of neighbouring nodes. The plural enlarged regions may be substantially equi-spaced around the boundary. Indeed, there may be plural groups of two or more enlarged regions and the groups may be substantially equi-spaced around the boundary.

In other embodiments, the enlarged regions may not be equally spaced around the boundary and the boundary, may have no rotational symmetry as such, or a reduced rotational symmetry compared with the characteristic rotational symmetry of the photonic band-gap structure. In this way, the overall structure may be rendered birefringent, for example if the enlarged regions are arranged to render the boundary two fold (or less) rotationally symmetric.

According to some embodiments, the nodes around the boundary are connected by relatively high refractive index veins. Then, a plurality of enlarged regions may be positioned along veins and spaced apart from any nodes.

The boundary region may comprise a nodule. The boundary region may comprise 2, 3, 4, 5, 6, 7, 8, 9 or more nodules, which may be arranged at regular intervals around the centre of the core. The nodules may be arranged at the centres of veins, where each vein extends between two nodes.

Alternatively, the nodules may be arranged off-centre on such a vein.

In another form, an enlarged region comprises a relatively thick vein, compared to the thickness of at least one other vein, extending between a pair of neighbouring nodes.

In yet another form the boundary may comprise at least one ridged region, characterised by plural enlarged regions in relatively close proximity. There may be plural ridged regions around the boundary. Indeed, a significant portion of the boundary may be ridged. In the limit, substantially the entire boundary may be ridged. The ridges may be on one or both peripheries of the boundary.

In some embodiments, at least one enlarged region is located on an outer periphery of the boundary. The enlarged region may resemble an outcrop or projection. In addition, or alternatively, at least one enlarged region may be located on an inner periphery of the

boundary. In some cases, there may be is at least one enlarged region on both the inner and outer peripheries of the boundary.

The microstructured region, in the plane cross section, may comprise a substantially periodic array of relatively low refractive index regions, being separated from one another by relatively high refractive index regions, the array having a characteristic primitive unit cell and a pitch Λ. For example, the microstructured region may comprise a substantially periodic, triangular array of relatively low refractive index regions. A primitive unit cell is a unit cell of the structure, having a smallest area (in the transverse cross section) that, by vector translations, can tile and reproduce the entire structure without overlapping itself or leaving voids. The pitch Λ is the minimum translation distance between two neighbouring primitive unit cells.

In some embodiments, the core is a seven cell defect (that is, it has a form that would result from omission or removal of relatively high refractive index regions from a first primitive unit cell and the six primitive unit cells that surround the first primitive unit cell of a triangular array of unit cells.

Alternatively, the core is a nineteen cell core defect (that is, it has a form that would result from omission or removal of relatively high refractive index regions from a first primitive unit cell, the six primitive unit cells that surround the first primitive unit cell and the twelve primitive unit cells that surround said six primitive unit cells, in a triangular array of unit cells.

Hitherto, the prior art teachings relating to PBG fibres have focused on a core defect that is just large enough to support a single mode, but not so large that it supports additional, unwanted modes. In practice, in the prior art, the preferred core defect size for fibres that have actually been made has generally been selected to be larger than a single unit cell but no larger than about the size of seven inner most capillaries, or unit cells, in a triangular array of capillaries. US patent application US6404966 purports to describe a single mode hollow core PBG fibre. However, it is unclear from the description how it would be possible to form a single mode PBG fibre having a large hollow core defect, particularly if the cladding has a pitch which is only half the optical wavelength.

As will be described herein, the present inventors have demonstrated that increasing the core defect size beyond sizes proposed in the prior art teachings may provide significant benefits, which potentially outweigh the perceived or actual disadvantages of doing so.

The present inventors also demonstrate that at least some of the perceived disadvantages of increasing the core defect size, based on well-understood theory for index-guiding fibres, do not necessarily apply in the case of PBG fibres. In addition, the present inventors propose that, to the extent certain perceived disadvantages of increasing the core defect size do exist, there are ways to mitigate these effects by careful design of the PBG fibre structure. A number of possible ways to mitigate such effects will be considered. In particular, the inventors demonstrate that the number and kinds of modes that are supported by a PBG fibre are not determined only by the diameter of the core defect, an index difference between a core and cladding and wavelength of light, unlike in a conventional index-guiding fibre. Indeed, the present inventors demonstrate herein that it is possible to increase the diameter of the core defect significantly without proportionately increasing the numbers of core modes supported by the PBG fibre. In addition, the present inventors show that core modes supported by the PBG fibre can be manipulated by varying only the form of the boundary region around the core.

The relatively low refractive index regions may be voids under vacuum or filled with air or another gas, for example N_2 or Ar.

At least some of the relatively high refractive index regions may comprise silica glass, for example pure or doped silica glass or other silicate glasses, although any other inorganic glass or organic polymer could be used in any practical combination.

At least some of the boundary veins may be substantially straight. Alternatively, or in addition, at least some boundary veins may be bowed inwardly or outwardly.

The microstructured region may comprise a photonic band-gap structure. Then, at least some of the enlarged regions may deviate from the form of the photonic band-gap structure. For example, there may be additional enlarged regions or the regions may be larger than would be expected from inspection only of the PBG structure.

Indeed, the boundary may have a different structure from the structure of the rest of the outer structure. For example, the regions of relatively high refractive index in the boundary region may be thicker or thinner than corresponding regions in the rest of the outer structure. The regions of relatively high refractive index may include nodes or nodules that are in different positions or have different sizes from corresponding features in the rest of the outer structure (it may be that there are no corresponding features in the outer structure or that there are such features in the outer structure but they are not present in the boundary region). The regions of relatively high refractive index in the boundary region may include a region of

a different refractive index from the refractive index of corresponding region in the outer structure.

It is highly unlikely in practice that a photonic bandgap structure according to embodiments of the present invention will comprise a 'perfectly' periodic array, due to imperfections being introduced into the structure during its manufacture and/or perturbations being introduced into the array by virtue of the presence of the core defect and/or additional layers (over-cladding) and jacketing around the photonic band-gap structure. The present invention is intended to encompass both perfect and imperfect structures. Likewise, any reference to "periodic", "lattice", or the like herein, imports the likelihood of imperfection.

Even if the outer structure is not a photonic bandgap structure, any features set out above in relation to other aspects of the invention having a bandgap structure may be found in the present further aspect of the invention unless that is not physically meaningful.

In addition, core boundaries having the aforementioned (and respective following) form may be used in combination with periodic or non-periodic photonic band-gap structures. Although periodic arrays are more common for forming a photonic band-gap, in principle, the array need not be periodic – see, for example, "Antiresonant reflecting photonic crystal optical waveguides", by N. M. Litchinitser et al., Optics Letters, Volume 27, No. 18, September 15, 2002, pp1592-1594. Although this paper does not provide calculations explicitly for PBG fibres, it does illustrate that photonic bandgaps may be obtained without periodicity.

An enlarged region may be coincident with a node such that the node appears to have an uncharacteristic form relative to the photonic band-gap structure. Typically, nodes or the like in prior art PBG fibre structures have a form that is substantially dictated by the form of the PBG cladding structure or the process used to make the PBG structure. In particular, in the prior art nodes tend to have a similar size and form as the other node-like formations in the PBG cladding structure. According to some embodiments of the present invention, however, the nodes that appear to have an uncharacteristic form may, by design, be larger, smaller or generally have a different form than the cladding nodes.

The proportion by volume of relatively low refractive index regions in the microstructured region may be greater than 75%. For example, it may exceed 80%, 85% or even 90%.

In preferred embodiments of the present invention, the waveguide supports a mode in which greater than 95% of the mode power in the waveguide is in relatively low refractive

index regions. In some embodiments, more than 98% or even 99% of the mode power is in the relatively low refractive index regions.

Typically, the waveguide supports a mode having a mode profile that closely resembles the fundamental mode of a standard, single mode optical fibre. This mode may support a maximum amount of the mode power in relatively low refractive index regions compared with other modes that are supported by the waveguide.

In addition, or alternatively, the waveguide supports a core-guided, non-degenerate mode. This mode may be the lowest loss mode of the waveguide. Alternatively, the fundamental-like mode may be the lowest loss mode of the waveguide.

In general, at least for larger core sizes (for example seven cell core defects and larger) the waveguide supports plural core-guided modes.

The waveguide may have an operating wavelength, wherein the pitch of the microstructured region is greater than the operating wavelength.

According to a second aspect, the present invention provides an optical fibre comprising a waveguide described above as being in accord with the present invention.

According to a third aspect, the present invention provides a transmission line for carrying data between a transmitter and a receiver, the transmission line including along at least part of its length a fibre of the aforementioned kind.

According to a fourth aspect, the present invention provides a preform for a microstructured optical fibre waveguide, comprising a stack of parallel, first elongate elements supported, in the plane cross section, around an inner region, which is to become a relatively low refractive index core region when the preform is drawn into a fibre, the preform further comprising second elongate elements, also supported or situated around the inner region, said second elements being arranged to generate a core boundary, at the interface between the photonic band-gap cladding and the core, when the preform is drawn into fibre, the arrangement of second elements being such that the core boundary comprises at least one relatively enlarged region when the preform is drawn into fibre.

The preform may further comprise a third elongate element for supporting the first and second elongate elements around the inner region. The third elongate elements may be a solid member or it may have a bore.

At least some of the second elongate elements may be situated in interstitial regions that form between the first elongate elements and the third elongate element. The third

elongate element may have at least one elongate detent around its periphery and one or more of the second elongate elements are situated in the detent or detents.

At least some second elongate elements are attached to an outer periphery of the third elongate element. In addition, or alternatively, at least some second elongate elements are attached to an inner periphery of the third elongate element. Second elongate elements may be attached to both inner and outer peripheries of the third elongate element. In any case, there may be at least one second elongate element fused to the third elongate element.

In some embodiments, the third elongate element is pre-profiled, in the transverse cross section, to have around its periphery enlarged regions that constitute the second elongate elements.

In alternative embodiments, the third elongate element comprises an inner capillary within the bore of an inside an outer capillary, and at least some second elongate elements are situated in a region that is formed between the inner capillary and the outer capillary.

In preferred embodiments, said first elongate elements are arranged, on a macro scale, to become a photonic band-gap cladding structure when the preform is drawn into a fibre. Then, the arrangement of second elongate elements may deviate from the arrangement of first elongate elements required to form the photonic band-gap cladding structure.

At least some of the second elongate elements may comprise solid rods. In addition, or alternatively, at least some of the second elongate elements may comprise capillaries. In some embodiments, the rods and/or capillaries may be the same size. In other embodiments, the rods and/or capillaries may be different sizes.

At least some of the first elements may have a circular cross section. At least some of the circular first elements may be capillaries. Then, said capillaries may be arranged in a triangular array. In addition, other first elongate elements may be solid rods that are situated in interstitial regions between the capillaries.

According to a further aspect, the present invention provides an optical fibre made from a preform as described hereinbefore as being in accord with the present invention.

According to a further aspect, the present invention provides a method of forming a photonic band-gap fibre, comprising the steps of forming a preform as described hereinbefore as being in accord with the present invention, and heating and drawing the preform, in one or more stages, into the fibre.

Brief Description of the Drawings

Embodiments of the present invention will now be described, by way of example only, with reference to the accompanying drawings, of which:

Figure 1 is a diagram of a transverse cross section of a PBG fibre structure of the kind known from the prior art;

Figure 2 is a diagram which illustrates how various physical characteristics of PBG fibres are defined herein;

Figures 3, 4 and 5 show diagrams of various examples of PBG fibre structures;

Figures 6 and 7 show mode spectra plots for the PBG fibre structures of Figures 3 and 4;

Figure 8 shows mode intensity distribution plots for a mode, supported by each structure of Figures 3 and 4, which supports the highest amount of light in air;

Figures 9 and 10 show graphs of mode intensity for x and y axes of the distributions of Figure 8;

Figure 11 shows mode spectra plots for the PBG fibre structures of Figure 5;

Figure 12, 13 and 14 show mode intensity distribution plots for a number of modes for each of the structures in Figure 5;

Figure 15 shows four alternative PBG fibre structures;

Figure 16 shows four further alternative PBG fibre structures;

Figure 17 is a diagram of a pre-form suitable for making PBG fibre according to the prior art;

Figure 18 is a diagram of a pre-form suitable for making a fibre according to examples of PBG fibres described hereinafter;

Figure 19 is an alternative pre-form suitable for making a fibre according to examples of PBG fibres described hereinafter;

Figure 20a is a photograph of a portion of a preform, according to an embodiment of the present invention, taken through a microscope;

Figure 20b is a scanning electron micrograph (SEM) image of a portion of a PBG fibre made using the preform of Figure 20a;

Figures 21 to 25 are diagrams of alternative pre-forms suitable for making fibres according to embodiments of the present invention;

Figure 26 is a diagram of an outer region of a pre-form stack according to embodiments of the present invention, wherein the stack is contained in a large, thick-walled

capillary and interstitial regions between the inner surface of the large, thick-walled capillary and the stack contain various sizes of solid packing rod; and

Figure 27 is a diagram of an exemplary transmission system which can use a PBG fibre according to embodiments of the present invention.

Best Mode For Carrying Out the Invention, & Industrial Applicability

Figure 1 is a representation of a transverse cross-section of a fibre structure of the kind described in the prior art and is used herein as a reference against which the characteristics of other structures described herein are compared. In the Figure, the black regions represent fused silica glass and the white regions represent air holes in the glass. As illustrated, the cladding 100 comprises a triangular array of generally hexagonal cells 105, surrounding a seven-cell core defect 110. A core defect boundary 145 is at the interface between the cladding and the core defect. The core defect boundary has twelve sides – alternatin g between six relatively longer sides and six relatively shorter sides - and is formed by omitting or removing seven central cells; an inner cell and the six cells that surround the inner cell. The cells would have typically been removed or omitted from a pre-form prior to drawing the pre-form into the fibre. As the skilled person will appreciate, although a cell comprises a void, or a hole, for example filled with air or under vacuum, the voids or holes may alternatively be filled with a gas or a liquid or may instead comprise a solid material that has a different refractive index than the material that surrounds the hole. Equally, the silica glass may be doped or replaced by a different inorganic glass or other suitable material such as an organic polymer.

Two longitudinal planes through the fibre structure of Figure 1 are denoted y and x; with y being a vertical plane passing through the centre of the structure and x being a horizontal plane passing through the centre of the structure as shown.

Hereafter, and with reference to Figure 1, a region of glass 115 between any two holes is referred to as a "**vein**" and a region of glass 120 where veins meet is referred to as a "**node**".

The core defect boundary 145 comprises the inwardly-facing veins of the innermost ring of cells that surround the core defect 110.

In practice, for triangular array structures that have a large air-filling fraction, for example above 75%, most of the cladding holes 105 assume a generally hexagonal form, as shown in Figure 1, and the veins are generally straight.

Figures 2a and 2b are diagrams which illustrate how various dimensions of the cladding structure of Figure 1 are defined herein, with reference to four exemplary cladding cells 200.

For the present purposes, a node 210' in the cladding, which is referred to herein as a "**cladding node**", is said to have a diameter measurement **d** defined by the largest diameter of inscribed circle that can fit within the glass that forms the node. A vein 205 in the cladding, which is referred to herein as a "**cladding vein**", has a length **l**, measured along its centre-line between the circles of the cladding nodes 210 & 210' to which the cladding vein is joined and a thickness, **t**, measured at its mid-point between the respective cladding nodes. Generally, herein, veins increase in thickness towards the nodes to which they are joined.

The mid-point of a cladding vein is typically the thinnest point along the vein. Unless otherwise stated herein, generally, a specified vein thickness is measured at the mid-point of the vein between the two nodes to which the vein is joined.

According to Figure 2, a cladding node is surrounded by three notional circular paths 215, each one being positioned between and abutting a different pair of neighbouring cladding veins that join the node. These three paths, in effect, define the 'roundness' of the corners of the cladding holes and abut the notional inscribed circle that defines the diameter of the respective node. More particularly, the periphery of the node between each pair of veins is defined by the portions of the circular paths 215 which begin at a point p and end at a point q along first and second veins respectively. Points p and q are equidistant from the centre of the node 210'. It will be appreciated that the diameter, d, of the node 210' is a function of the thickness, t, of the veins, the distance of p from the centre of the node and the pitch Λ, or centre to centre distance between neighbouring cells, of the structure.

The cells forming the innermost ring around the boundary of the core defect, which are referred to herein as "**boundary cells**", have one of two general shapes. A first kind of boundary cell 125 is generally hexagonal and has an innermost vein 130 that forms a relatively shorter side of the core defect boundary 145. A second kind of boundary cell 135 has a generally pentagonal form and has an innermost vein 140 that forms a relatively longer side of the core defect boundary 145.

There are twelve boundary cells 125, 135 and twelve nodes 150, which are referred to herein as "**boundary nodes**", around the core defect boundary 145. Specifically, as defined herein, there is a boundary node 150 wherever a vein between two neighbouring boundary cells meets the core defect boundary 145. In Figure 1, these boundary nodes 150 have

slightly smaller diameters than the cladding nodes 160. Additionally, there is an enlarged region 165, or "**bead**", of silica at the mid point of each relatively longer side of the core defect boundary 145. These beads 165 coincide with the mid-point along the inner-facing vein 140 of each pentagonal boundary cell 135. The beads 165 may result from a possible manufacturing process used to form the structure in Figure 1, as will be described in more detail below. For the present purposes, the veins 130 & 140 that make up the core defect boundary are known as "**boundary veins**".

As will be described below, it is possible to control the diameters of particular nodes and the existence or size of beads along the core defect boundary during manufacture of a fibre.

The structure in Figure 1 and each of the following examples of different structures closely resemble practical optical fibre structures, which have either been made or may be made according to known processes or the processes described hereinafter. The structures share the following common characteristics:

a pitch Λ of the cladding chosen between values of approximately 3μm and 6μm (this value may be chosen to position core-guided modes at an appropriate wavelength for a particular application);

a thickness t of the cladding veins of 0.0586 times the chosen pitch Λ of the cladding structure (or simply 0.0586Λ);

an AFF in the cladding of approximately 87.5%; and

a ratio **R** having a value of about 0.5.

Referring to Figure 2, **R** is defined as the ratio of the distance of p' from the centre of the nearest cladding node to half the length of a cladding vein, **l/2**; where p' is a point along the centre-line of a cladding vein and is defined by a construction line that passes through the centre-line of the vein, the centre of circle 215 and the point p where the circle meets the vein.

In effect, R is a measure of the radius of curvature of the corners of the hexagonal cells within the cladding. It will be apparent that the maximum practical value of R is 1, at which value the radius of curvature is a maximum and the cladding holes are circular. The minimum value of R is dictated by the thickness t and length l of the veins and is the value at which the diameter of the circle 215 tends to zero and the cladding holes are hexagonal.

For all values of R below the maximum value, the veins appear to have a region of generally constant thickness about their mid-points, which increases in length with decreasing R. For example, a value of R=0.5 provides that around half the length of a vein, about its

mid-point, has a substantially constant thickness. Likewise, a value of R=0.25 provides that around three quarters of the length of a vein, about its mid-point, has a substantially fixed thickness.

Given R, t and Λ, for practical purposes, the diameter d of the cladding nodes is found to be approximately:

$$d = \frac{2R\Lambda}{\sqrt{3}} - \Lambda R + t \qquad \text{(Equation 1)}$$

In Figure 1, the diameter of each boundary node 150, d_e, is smaller than the diameter of the cladding nodes 160, due to there being less glass available at the boundary for forming the nodes. A model similar to that shown in Figure 2 may if required be used to define the form of the boundary nodes. The differences between Figure 2 and the model for the boundary nodes are (1) the boundary node model includes the core defect 110 and two boundary cells rather than three cladding cells, (2) it is assumed that the value of R is a minimum, such that there is no measurable circular path inside the core defect 110; and, (3) the internal angles of the core defect and the boundary cells are different from each other and from the cells in the cladding.

The beads 165 shown in Figure 1 are substantially oval shaped, each having a major dimension which is approximately 1/3 the length of the distance between the two node centres that lie on either side of the bead and a minor dimension which is 1/3 the length of the major dimension. The minor dimension of the bead, which defines the thickness of the associated vein at its mid-point, is slightly longer than the diameter of the respective boundary nodes 150.

For boundary veins with no beads, the thickness at the mid-point of the vein between boundary nodes is the same as the thickness of the cladding veins at the same point.

The present inventors have determined that it is possible to control the performance of PBG fibres in particular by aiming to maximise the amount of light that propagates in air within the fibre structure, even if some light is not in the core, in order to benefit from the properties of PBG fibres, such as reduced absorption, non-linearity and, in addition, reduced mode coupling.

For the purposes of comparing aspects of the performance of various different structures it is useful to consider the modes that are supported in the band gap of various PBG

fibre structures. This may be achieved by solving Maxwell's vector wave equation for the fibre structures, using known techniques. In brief, Maxwell's equations are recast in wave equation form and solved in a plane wave basis set using a variational scheme. An outline of the method may be found in Chapter 2 of the book "Photonic Crystals – Molding the Flow of Light", J.D. Joannopoulos et al., ©1995 Princeton University Press.

Figures 3 and 4 illustrate six exemplary PBG fibre structures that will be considered hereafter. Figure 3 illustrates three structures identified as S1, S2 and S3 herein, which are seven-cell core defect structures. S1 is the same as the structure illustrated in Figure 1 and is reproduced in Figure 3 for convenience only. S2 and S3 reinforce various characteristics of the invention, as determined by the present inventors, and, in particular, are discussed herein in order to illustrate how the mode spectrum of a given structure may vary significantly without varying the size of the core defect but, instead, varying different core defect boundary characteristics.

Figure 4 illustrates three structures identified as S4, S5 and S6, each having a nineteen-cell core defect. S4 is an exemplary embodiment of the present invention. S4, S5 and S6, apart from core defect size, have the same cladding characteristics as S1, S2 and S3 respectively. S1 to S3 have a maximum core defect radius of about 1.5Λ. In contrast, S4 to S6 have a maximum core defect radius of about 2.5Λ.

The characteristics of structures S2 to S6 will now be described in further detail.

There are a number of differences between the form of the core defect boundary in S1 and the boundary in S2. S2 has reduced boundary node diameters, which are significantly smaller than the cladding nodes 360, compared with S1, and no apparent beads along the core defect boundary 345. According to the definitions provided herein, the boundary nodes 355 in S2 have a minimum diameter; the associated values of R are at a minimum and, accordingly, there are no measurable circular paths defining the periphery of the nodes. The diameters of the boundary nodes 355 in S2 are only very slightly larger than the thickness of the boundary veins 330, 340. In contrast, as for S1, the cladding nodes 360 have diameters that are significantly larger than the thickness of their adjoining veins 315.

It may in practice be difficult to make the exact structure of S2 due to surface tension effects acting on the glass during the drawing process, which may cause the cladding veins to meet the boundary veins at slightly rounded corners; meaning R is not its theoretical minimum. However, it is useful to compare the characteristics of S2 with the other structures

herein. Structures closely resembling S2, however, can be made according to a method that will be described in detail below.

The boundary in S3 has no apparent beads, as in S2, and the boundary nodes 355 have a similar diameter to those in S1.

The structure in S4 has an additional ring of cladding cells removed from around the core defect compared with S1. This forms a core defect 410 equivalent to nineteen missing cladding cells. Similar to S1, S4 has boundary nodes 450 that are significantly larger in diameter than the thickness of the respective boundary veins and there are hexagonal cells 425 at each corner of the core defect 410. However, in contrast to S1, which has one generally pentagonal cell along each side of the core defect boundary 145, S4 has two generally pentagonal cells 435 along each side of the core defect boundary 445. In addition, there are two beads 455 along each side of the core defect boundary 445, roughly coincident with the mid-point of the vein 440 of each pentagonal cell 425 that borders the core defect boundary 445. The minor dimension of each bead is slightly longer than the diameter of the nodes to which each respective vein is joined. There are also three boundary nodes 455 per relatively longer side of the core defect boundary 445, compared with two for the seven-cell core defect structures. Overall, S4 has eighteen cells sharing veins with the core defect boundary 445. S4 represents an exemplary embodiment of the present invention.

The boundary in S5 is similar to S2 in the respect that it has reduced-diameter boundary nodes 455', which do not have diameters that are significantly larger than the thickness of the respective veins, and there are no apparent beads. All other parameters of S5 are the same as S4. S5 represents an exemplary embodiment of the present invention.

The boundary in S6 has no apparent beads, as in S3, and the boundary nodes 455 have a similar diameter to those in S1. All other parameters of S6 are the same as S4. S6 represents an exemplary embodiment of the present invention.

Figure 5 illustrates three further nineteen-cell core defect structures, S7, S8 and S9, which have cladding arrangements very similar to those of structures S4-S6. The latter two structures are embodiments of the present invention. Structure S7 has no beads around the core defect boundary, S8 has enlarged beads around the core defect boundary (compared with the beads in S4) and S9 has two smaller beads in place of the single beads per vein of S8. Structures S8 and S9 are embodiments of the present invention.

Figures 6 and 7 each show three mode spectra, identified as P1 to P3 and P4 to P6 respectively. Each spectrum P1 to P6 relates to a respective PBG fibre structure S1 to S6.

The horizontal axis of each spectrum is normalised frequency, $\omega\Lambda/c$, where ω is the frequency of the light, Λ is the pitch of the cladding structure, and c is the speed of light in a vacuum. The vertical axis of each spectrum relates to the response of the structure to a given input for a given normalised wave-vector $\beta\Lambda=13$, against which the spectrum is plotted, where β is the chosen propagation constant for the calculations. The spectra are produced using a Finite-difference Time Domain (FDTD) algorithm, which computes the time-dependent response of a given hollow core structure to a given input. This technique has been extensively used in the field of computational electrodynamics, and is described in detail in the book "Computational Electrodynamics: The Finite-Difference Time-Domain Method", A. Taflove & S.C. Hagness, ©2000 Artech House. The FDTD technique may be readily applied to the field of PBG fibres and waveguides by those skilled in the art of optical fibre modelling.

With reference to spectra P1 to P6, each vertical spike indicates the presence of at least one mode at a corresponding normalised frequency. In some cases, multiple modes may appear as a single spike or as a relatively thicker spike compared with other spikes in a spectrum. This is due to the fact that the data used to generate the spectra is not of a high enough resolution to distinguish very closely spaced modes. As such, the mode spectra should be taken to provide only an approximation to the actual numbers of modes that exist for each structure, which is satisfactory for enabling a general comparison between spectra herein.

On each spectrum, a 'light line' for the respective structure is shown as a solid vertical line at $\omega\Lambda/c=13=\beta\Lambda$, and band edges, which bound a bandgap, are represented as two dotted vertical lines, one on either side of the light line, with a lower band edge of the bandgap at around $\omega\Lambda/c=12.92$ and an upper band edge of the bandgap at around $\omega\Lambda/c=13.30$. A bandgap in P1 to P6 is a range of frequencies of light for a given β. For the present examples, the bandgap is slightly wider than 0.35 (in units of $\omega\Lambda/c$). The inventors estimate that the minimum practical width for a PBG fibre bandgap would be around 0.05 in the present units of measure but, more preferably, would be greater than 0.1.

Modes that are between the light line and the lower band edge (that is, to the left of the light line) will concentrate in the glass and be evanescent in air whereas the modes that are between the light line and the upper band edge (that is, to the right of the light line) may be air-guiding.

As shown in P1, relating to S1, there are around three modes between the light line and the lower band edge and around nine modes between the light line and the upper band

edge (taking the thicker spikes as two modes). It is clear that S1 supports a significant number of modes, some of which could be air-guiding; although, it is unlikely that all of these modes will be excited by a given light input. Analysis of the individual modes shown in the bandgap of P1 leads to a finding that the mode marked as F1 is an air-guiding mode, which most closely resembles the form of a fundamental mode in a typical standard optical fibre and supports the maximum amount of light in air. The mode is found to be degenerate, being one of a pair of very similar modes falling at about the same position in the bandgap.

As shown in P2, relating to S2, approximately two modes lie between the light line and the lower band edge and there are around twelve modes between the light line and the upper band edge. As with S1, S2 supports a significant number of modes, some of which could be air-guiding. The mode marked F2 in P2 is found to be a degenerate, air-guiding mode that most closely resembles the form of a fundamental mode in a typical standard optical fibre and supports the maximum amount of light in air.

The structural characteristics of S2 are not that different from those of S1; the only differences being the reduced boundary node sizes in S2 and omission of the beads. Notably, the core defect diameters of the two structures are the same. However, the mode spectra for the two structures are significantly different, there being more potentially-air-guiding modes supported by S2 but fewer modes that are evanescent in air.

As shown in P3, relating to S3, there are around three modes between the light line and the lower band edge and around thirteen modes between the light line and the upper band edge. Again, it is clear that S3 supports a significant number of modes, some of which could be air-guiding. The mode marked F3 in P3 is a degenerate, air-guiding mode that most closely resembles the form of a fundamental mode in a typical standard optical fibre and supports the maximum amount of light in air.

Again, the structural characteristics of S3 are only subtly different from those of either S1 or S2, with the core defect diameters of all structures being the same. However, the mode spectrum for S3 is, once more, significantly different from the mode spectra of either S1 or S2.

As shown in P4, relating to S4, which is a nineteen-cell core defect structure, there are approximately two to four modes between the light line and the lower band edge and in excess of twenty modes between the light line and the upper band edge of the bandgap region. Clearly, S4 appears to support significantly more modes than any of the foregoing seven-cell core defect structures. The mode marked F4 in P4 is again a degenerate, air-guiding mode

that most closely resembles the form of a fundamental mode in a typical standard optical fibre and supports the maximum amount of light in air.

The core defect diameter of S4 is significantly larger than in S1, whereas the other parameters are substantially the same. On the basis of prior art thinking it is not a surprise that there appear to be significantly more modes supported in the nineteen-cell core defect structure of S4 than in any of the seven-cell core defect structures S1 to S3.

As shown in P5, relating to S5, there are approximately four modes between the light line and the lower band edge and around fifteen to twenty modes between the light line and the upper band edge. Again, S5 appears to support significantly more modes than the foregoing seven-cell core defect structures. The mode marked F5 in P5 is a degenerate, air-guiding mode that most closely resembles the form of a fundamental mode in a typical standard optical fibre and supports the maximum amount of light in air.

The mode spectra for S4 and S5 are similar in terms of numbers of modes, with both structures supporting a number of evanescent and possibly air-guiding modes.

As shown in P6, relating to S6, there is a single mode between the light line and the lower band edge and approximately twelve to fifteen modes between the light line and the upper band edge. Thus, S6 appears to support significantly fewer modes than either of S4 or S5, even though the core defect sizes are the same. Surprisingly, the mode spectrum of S6 appears to resemble, in both numbers and positions of modes, the mode spectrum of S2, which is a seven-cell core defect structure. This is contrary to prior art thinking, which indicates that larger core defects should support, proportionately, more modes. The mode marked F6 in P6 is again a degenerate, air-guiding mode that most closely resembles the form of a fundamental mode in a typical standard optical fibre and supports the maximum amount of light in air.

On the basis of the above six examples of different PBG fibre structures, it is clear that the numbers and locations of modes in a mode spectrum are not determined only by size of the core defect, index difference between a core and cladding and wavelength of light; even when the cladding structure is fixed. Taking S1 to S3, for example, it is clear that the locations of modes and, in particular, the number of modes that are likely to be evanescent in air or possibly air-guiding, can be varied significantly by varying the node size, and presence or absence of beads, about the core defect boundary, without the need to vary the core defect size. Additionally, while certain PBG fibre structures that support a greater number of modes – especially potentially air-guiding modes – may be made by increasing the core defect size

for any given cladding structure, it also appears possible to increase the core defect size without significantly increasing the number of modes that are supported by the structure. This is surprising and contrary to the thinking in the prior art.

Figure 8 comprises six plots, D1 to D6, which show the mode intensity distributions, over a transverse cross-section of a respective PBG fibre structure, for modes F1 to F6 respectively. The shading of the plots is inverted, such that darker areas represent more intense light than lighter regions. Each plot shows the position and orientation of x and y planes, which correspond to the x and y planes of the structures, as illustrated in Figures 3 and 4. These plots were produced using the results obtained by solving Maxwell's equations for each structure, as described above.

The graphs in Figures 9 and 10 show the mode intensity for modes F1 to F6 along longitudinal planes x and y of D1 to D6 respectively. The intensity values are normalised so that the maximum intensity of the mode is at 0dB on the graph; the y-axis scale being logarithmic. The shaded vertical lines and bands across the graphs coincide with and represent the glass regions of the actual respective structure along the x and y planes. For the x and y planes, therefore, it is possible to see how the light intensity of the mode varies in the air and glass, and across the glass/air boundaries, of each structure.

Table 1 below shows, for modes F1 to F6, the approximate normalised frequency at which the mode lies within the bandgap of its respective structure and the percentage of light that is in air rather than in the high index silica regions.

Mode Number	Normalised frequency ($\omega\Lambda/c$)	% light in air
F1	13.14	92.8
F2	13.12	97
F3	13.11	97.5
F4	13.05	97.7
F5	13.04	99.6
F6	13.04	99.5

Table 1

The percentage of light in air for modes is found by calculating the integral of the light intensity across only the air regions of the plots in Figure 8 and normalising to the total power. Of course, the plots in Figure 8 represent the intensity across only an inner region of the

various PBG fibre structures. Accordingly, the respective percentages of light in air are calculated for the inner regions only and may be slightly different if calculated across entire PBG fibre structures instead. However, as will be seen, the intensities have typically reduced so considerably towards the edges of the plots that any light in regions outside of the inner regions, whether in air, glass or both, is unlikely to have any significant impact on the percentage of light in air values.

Plot D1 shows the mode intensity distribution for the F1 mode, which was found at a normalised frequency $\omega\Lambda/c$ of about 13.14. Plot D1 together with graphs x1 and y1 show that the F1 mode has a generally circular central region in the core defect. The central region of the mode is intense at its centre and decays sharply towards the core defect boundary. There are two intense satellites to the left and right of the central region, coincident with the core defect boundary, and a number of less intense satellites that form a broken ring around the central region. As shown in graph x1, the satellites to the left and right of the central region have slightly higher intensities than the maximum intensity of the central region. It is significant to note that these intense satellites, along with the larger ones of the less intense satellites around the boundary, appear to coincide with the beads of S1. In addition, it would appear that the remainder of the less intense satellites appear to coincide with the boundary nodes of S1. There is evidence in D1 of some light being concentrated further out from the centre of the structure than the core defect boundary although, as is supported by graphs x1 and y1, the light intensity drops-off rapidly away from the central region. The light that is outside the core defect appears to coincide with cladding nodes.

It is apparent that, for the seven-cell core defect structure S1, a significant amount of light concentrates in the pronounced beads. It is apparent, however, that the F1 mode is air-guiding, with a significant fraction of the light existing in the core defect and with a local intensity minimum of the mode falling within the core defect boundary. The intensity of the light in the glass of the cladding structure decreases significantly moving further away from the core defect boundary.

Plot D2 shows the mode intensity distribution of the F2 mode in the transverse plane of S2. The mode was found at a normalised frequency $\omega\Lambda/c$ of about 13.12. Plot D2 together with graphs x2 and y2 show that the F2 mode has a generally circular central region in the core defect. The central region is intense at its centre and decays sharply towards the core defect boundary. There are six relatively lower intensity satellites about the central region, coincident with the core defect boundary, and lower intensity satellites in glass further out

from the central region. The six satellites around the core defect boundary have a lower intensity than the maximum intensity of the central region, in contrast to the intense satellites of plot D1. It is believed that in plot D2 the intensities of the satellites around the core defect boundary are less than in plot D1 due to the removal of the pronounced beads; in-keeping with the observation that, for a seven-cell core defect structure, a significant amount of light concentrates in the pronounced beads.

As with the F1 mode, it is apparent that the F2 mode is air-guiding. It is also apparent that some of the light concentrates in the glass of the cladding structure.

The percentage of light in air for the F2 mode is 97%. This value is significantly larger than the value of 92.8% for the F1 mode even though the core defect size is the same. This increase in the amount of light in air is attributed to the reduction in diameter of the boundary nodes and omission of the beads. Accordingly, it is expected that S2 will have improved loss, non-linearity and mode coupling characteristics compared with S1.

Plot D3 shows the mode intensity distribution of the F3 mode in the transverse plane of S3. The mode was found at a normalised frequency $\omega\Lambda/c$ of about 13.11. The qualitative and quantitative characteristics of the F3 mode, as shown in plot D3 and graphs x3 and y3, very closely match those of the F2 mode. Similarly, the value of the percentage of light in air for the F3 mode is 97.5%, which is very close to the figure for the F2 mode. Accordingly, it is expected that S3 will also have improved loss, non-linearity and mode coupling characteristics compared with S1.

Plot D4 shows the mode intensity distribution of the F4 mode in the transverse plane of S4. The mode was found at a normalised frequency $\omega\Lambda/c$ of about 13.05. Plot D4 together with graphs x4 and y4 show that the F4 mode has a generally circular central region in the core defect. The central region is intense at its centre and decays rapidly towards the core defect boundary, although not as rapidly as in Plots D1 to D3. The central region has a local minimum that falls close to and within the core defect boundary, which means that the central region of the mode in plot D4 has a diameter in the order of two pitches longer than for any of the seven-cell core defect structures.

There are a number of low intensity satellites around the central region in plot D4, which appear to coincide with the boundary nodes of S4. From graphs x4 and y4, these satellites appear to be more than 20dB lower than the peak intensity of the central region. However, it should be noted that the x4 plane does not cross the core defect boundary at a bead, whereas planes x1 to x3 do, which means it is not possible to make a direct comparison

of satellite intensity between graph x4 and graphs x1 to x3. The fact that the satellites in plot D4 appear so faint, though, does indicate that they have a significantly reduced intensity compared with satellites in plots D1 to D3.

The F4 mode is apparently air-guiding, with a significant fraction of the light existing in the core defect. Light which is guided outside of the core defect is concentrated in the glass. The percentage of light in air for S4 is 97.7%. This value is an improvement over the highest seven-cell core defect structure value by a small margin (0.2%) and a significant improvement (4.9%) over S1, which has a similar boundary node configuration. Accordingly, it is expected that S4 will have improved loss, non-linearity and mode coupling characteristics compared with S1.

Plot D5 shows the mode intensity distribution of the F5 mode in the transverse plane of S5. The mode was found at a normalised frequency $\omega\Lambda/c$ of about 13.04. Plot D5 together with graphs x5 and y5 show that the F5 mode is very similar in form to the F4 mode, with an intense central region and only very faint satellites outside of the central region. These satellites appear fainter than those in plot D4. Like the F4 mode, it is apparent that the F5 mode is air-guiding with a significant fraction of the light existing in the core defect.

The percentage of light in air for the F5 mode is 99.6%, which is significantly higher than the value of 97.7% for the F4 mode, even though the core defect sizes are the same. This increase in light in air value is attributed to the reduction in size of the boundary nodes and omission of the beads in S5 when compared with S4. It is expected that S5 will have significantly improved loss, non-linearity and mode coupling characteristics compared with S1 and S4.

Plot D6 shows the mode intensity distribution of the F6 mode in the transverse plane of S6. The mode was found at a normalised frequency $\omega\Lambda/c$ of about 13.04. Plot D6 together with graphs x6 and y6, relating to the F6 mode, very closely match the qualitative and quantitative characteristics of the F5 mode. In addition, the percentage of light in air for the F6 mode is 99.5%, which is similar to the value for the F5 mode. Accordingly, like S5, it is expected that S6 will have significantly improved loss, non-linearity and mode coupling characteristics compared with S1 and S4, while at the same time not supporting a significantly increased number of modes compared with the seven-cell core defect structures of Structures S1 to S3.

Table 2 below provides data for six further exemplary waveguide structures, S10 to S15. The waveguide structures for S10-S15 very closely resemble S3, in that the boundaries

have no apparent beads and the boundary nodes have a similar diameter to those in S1. Due to the similarity, and for reasons of brevity herein, S10-S15 are not independently represented in the Figures. The difference between the structures is only in boundary vein thickness, as shown in Table 2. The variations in boundary vein thickness are compensated for by slight variations in core defect diameter.

In Table 2, boundary vein width is normalised relative to the pitch Λ of the structures, which was the same for each structure. Structure S10 has a boundary vein thickness the same as the cladding vein thickness and, hence, was closest in form to S3. For each structure, the position of the mode having the highest percentage of light in air is presented as a frequency that is normalised with respect to the pitch of the structure.

Structure	Boundary Vein Width/Λ	Normalised frequency ($\omega\Lambda/c$)	% light in air
S10	0.0383	13.11	98.6
S11	0.0438	13.11 (13.29)	98.2 (97.7)
S12	0.0493	13.10	96
S13	0.0548	13.12 (13.28)	96.9 (98.3)
S14	0.0602	13.11	97.3
S15	0.0657	13.11	97.8

Table 2

Discounting for the moment the values in parentheses in Table 2, the modes having the highest percentage of light in air for each structure were found to be ones which most closely resemble the fundamental mode in a standard optical fibre communications system. As can be seen, varying the width of the boundary veins has little effect on the position of the respective modes. In contrast, however, variation in boundary vein thickness has a significant impact on the percentage of light in air for the modes. Within the coarse range of boundary vein thicknesses examined, it can be seen that a candidate as a preferred structure in terms of maximum light in air is S10, which has a boundary vein thickness of around 0.0383Λ (around 70% of the cladding vein thickness). However, a significant improvement over S13 is also seen at a boundary vein thickness of around 0.0438Λ (around 80% of cladding vein thickness). It is worthy of note, also, that the improvement is not linear, with the boundary vein thickness of S12 (around 90% of cladding vein thickness) producing a lower percentage

of light in air than either of S13 or S11. In addition, slight improvements over S13 are seen with S14 and S15, which have thicker boundary veins than S13.

Although not described herein in detail, the inventors have found that the mode spectra for structures S10 to S15 vary considerably with varying boundary vein thickness. The variations were at least as marked as those found by varying the boundary node size and bead presence in structures S1 to S3, which are very similar seven-cell core defect structures.

Turning now to the values in parentheses in Table 2, for structure S13, a mode having the values shown was found to be non-degenerate and to exist within the bandgap of S13 to the right of the light line. This mode was found to support the highest fraction of light in air for the structure.

All other modes, which have been shown herein to support the maximum fraction of light in air, have been degenerate.

As will be appreciated, a non-degenerate mode may find beneficial application, for example, in a system that is required to have minimal polarisation mode dispersion. This is because, once light has been launched or coupled into the non-degenerate mode, there is no scope for power to couple between degenerate mode pairs, which is the cause of such dispersion in practical systems.

The mode represented by the values in parentheses for S11 was also found to be non-degenerate. However, for this structure, the value of percentage of light in air for this mode was less than the value for the mode that most closely resembles the form of a fundamental mode.

It is expected that there are likely to be a number of non-degenerate modes supported by the present waveguide structures, as will be described hereinafter. However, whether or not the modes exist within the bandgap of a particular structure would depend on the relationship between the bandgap and the respective mode spectrum, which, as has been shown, can be extremely sensitive to core size and boundary form at least. The non-degenerate modes typically exist at higher frequencies than the fundamental-like modes. Similarly, the present inventors have found that nineteen cell core defect structures also support these non-degenerate modes.

Mode spectra P7-P9 for respective structures S7 to S9 are shown in Figure 11. In these spectra, the modes numbered 1 and 2 are degenerate, fundamental-like modes supported by the structure and the other numbered modes are the modes that are nearest to the fundamental modes. Each of the numbered modes has a respective mode intensity plot,

identified as Dn-m in Figures 12 to 14 (where n is the structure number and m is the mode number).

Spectra P7, relating to S7, has a degenerate pair of fundamental modes D7-1 and D7-2 just to the right of the light line. To the right of the fundamental modes is a single mode D7-5, which can be identified as a so-called 'surface mode', which has a significant portion of its power in or near to the core defect boundary. Further to the right is a group of three core guided modes, D7-6 to D7-8. Further to the right is another surface mode D7-9. To the left of the light line, but still within the bandgap, are two surface modes D7-3 and D7-4. As can be seen, the fundamental modes in this spectrum P7 are reasonably well spaced from the other modes that are supported within the bandgap.

Spectrum P8, relating to S8, has the same degenerate pair of fundamental modes D8-1 and D8-2 just to the right of the light line. In this case, however, there is a group of four modes: two non-degenerate modes D8-5 and D8-8, resembling the TM_{01} and TE_{01} modes of a standard optical fibre, and a degenerate pair of similar looking modes D8-6 and D8-7, which resemble the HE_{21} modes of a standard optical fibre. This group is further away from the fundamental modes that in P7. Just to the left of the fundamental modes, but still to the right of the light line, are three surface modes; D8-3, D8-4 and D8-9.

Spectrum P9, relating to S9, shows the two fundamental modes D9-1 and D9-2, closely surrounded on both sides by surface modes D9-3-D9-6.

From the mode spectra results for structures S7-S9 it is clear that it is possible to vary quite dramatically the modal characteristics of a given structure by adjusting only the core boundary characteristics thereof. In particular, while structure S8 has a relatively good spacing of modes from the fundamental pair structure, S9 has a number of surface modes in very close proximity to the respective fundamental pair. The present inventors expect, therefore, that structure S9 will experience far more loss due to mode coupling of power from the core modes to the boundary modes than either of S7 or S8 at the given operating wavelength.

The present inventors believe that slight variations on the core boundary have profound effects on the surface modes because these modes reside primarily in the glass of the core boundary. In contrast, slight variations in the core boundary are less likely to have an effect of the core modes, since very little of the light of these modes is in the core boundary.

In practical optical fibre transmission systems, it is expected that one fixed parameter will be operating wavelength. It is well-known that a PBG fibre can be designed for operation

at a given wavelength, for example at around 1550nm, since the dimensions of PBG structures simply scale with wavelength. However, the present inventors anticipate that there may be a need to tune a given PBG fibre structure, to optimise its performance at the given wavelength; for example, by manipulating the spectral positions of surface modes to move them away from the core modes of interest. Embodiments of the present invention find particularly beneficial application as a way of so tuning PBG fibres, independently or in addition to varying core diameter and other parameters of the fibres.

The structures illustrated in the diagram in Figure 15 are seven cell core defect structures according to embodiments of the present invention.

Figure 15a has a core boundary which includes six inwardly-facing nodules along the six relatively longer boundary veins. Figure 15b is a diagram of an alternative structure, having outwardly-facing nodules along six relatively shorter boundary veins. Figure 15c illustrates a similar structure, this time having alternating inwardly and outwardly facing nodules along the six relatively shorter boundary veins. Figure 15d has relatively thick boundary veins extending between pairs of neighbouring boundary nodes that coincide with hexagonal boundary cells. In this embodiment, the thickness of the thicker veins is about 2.5 times the thickness of the other boundary and cladding veins.

The structures illustrated in Figure 16 are yet further embodiments of the present invention. Figure 16a-16c are nineteen cell core defect structures. Figure 16a has a core boundary comprising eighteen boundary veins and every vein includes a bead. In contrast, Figure 16b has what might be considered a corrugated core defect boundary, since each boundary vein comprises a row of closely packed beads: six beads along each longer boundary vein and three beads along each shorter boundary vein. The structure in Figure 16c is similar to the structure in Figure 16b. However, in Figure 16c, the beads only project outwardly from the core defect boundary. It would of course also be possible to provide a similar structure in which the beads projected only inwardly from the core defect boundary. Figure 16d is an additional seven cell core defect structure, which has enlarged beads extending between respective pairs of more widely spaced neighbouring nodes.

With reference to Figure 17, prior art structures of the kind exemplified by S1 may be made from a pre-form 1700 comprising a stack of hexagonal capillaries 1705. The hexagonal capillaries 1705 each have a circular bore. The cladding nodes 160 and boundary nodes 150 (from Figure 1) of the PBG fibre structure result from the significant volume of glass that is present in the perform 1700 wherever the corners 1710, 1715 of neighbouring capillaries

meet. The beads 165 are formed from the glass of the inwardly-facing corners 1720 of the capillaries that bound an inner region 1725 of the pre-form 1700, which is to become the core defect region 170 of a PBG fibre structure. These corners 1720, and the two sides of each capillary that meet at the corners, recede due to surface tension as the stack of capillaries is heated and drawn. Such recession turns the two sides and the corner 1720 into a boundary vein 140, with a bead 165. The inner region 1725 may be formed by omitting the inner seven capillaries from the pre-form and, for example, supporting the outer capillaries using truncated capillaries at either end of the stack, as described in PCT/GB00/01249 (described above) or by etching away glass from inner capillaries in accordance with either PCT/GB00/01249 or US 6,444,133 mentioned above. In some prior art structures, the known beads may result from an etching process rather than being entirely due to use of hexagonal capillaries.

While it is possible to adapt the prior art processes in order to make the nineteen-cell core defect S4, which has beads on some of the boundary veins, the present inventors have appreciated that it would be more difficult to manufacture any of S5 or S9 using the prior art techniques. In particular, it would be difficult to control the diameters of boundary nodes using hexagonal cross section capillaries of the kind described with reference to Figure 17. On the other hand, it is difficult to make structures having cladding nodes with diameters which are significantly larger than their respective veins by using purely circular capillaries, especially when the required AFF is high, for example higher than 75%. In addition, formation of beads or nodules (or the like) at selected locations around the core boundary is difficult using prior art processes.

The diagram in Figure 18 illustrates one way of forming a pre-form stack 1800, including a nineteen cell core region 1810, which is suitable for forming a PBG fibre structure S4 or S8. The core region 1810 is formed by assembling circular cross section capillaries 1805 in a close-packed triangular arrangement around a large diameter core capillary 1815, which is large enough to support capillaries around a region left by removal of nineteen capillaries: an inner capillary, the six capillaries around the inner capillary and the twelve capillaries around the six capillaries. The cladding capillaries 1805 have an outer diameter of about 1mm and a wall thickness of about 0.05mm and the large diameter core capillary 1815 has an outer diameter of about 4.5mm and a wall thickness of about 0.05mm. The large diameter core capillary 1815 supports the cladding capillaries while the stack is being formed and eventually becomes part of the material that forms a core defect boundary.

Interstitial voids 1820 that form at the at the mid-point of each close-packed, triangular group of three cladding capillaries are each packed with a glass rod 1840, which has an outer diameter of about 0.15mm. The rods 1825 that are packed in voids assist in forming cladding nodes, which have a diameter d that is typically significantly greater than the thickness t of the veins that meet at the nodes. Omission of a rod from a void in the cladding leads to the formation of a cladding node that has a relatively smaller diameter, for example closer to the thickness of the respective adjoining veins.

The rods 1825 may be inserted into the voids after the capillaries have been stacked. Alternatively, the stack may be assembled layer by layer, with the rods that rest on top of capillaries being supported by an appropriate jig, for example positioned at either end of the stack, until the next upper layer of capillaries is in place to support those rods. In commercial scale operations, it is apparent that the manual task of forming a pre-form stack could readily be automated, using appropriately programmed robots, for example of the kind used in component laying for printed circuit boards.

The interstitial voids 1830 that are formed between the cladding capillaries 1805 and the large diameter capillary 1815 are not packed with any rods, thereby minimising the volume of glass that is available, during drawing of the stack 1800, for formation of boundary nodes.

As shown in Figure 18, the large diameter capillary 1815 has attached to its inner surface twelve silica rods 1835. The rods 1835 are fused to the inside of the large diameter capillary 1815 in an additional heating step before the capillary is introduced to the stack 1800. When the stack 1800 is heated and drawn into fibre, these rods fuse with the large diameter capillary 1815, which itself fuses to the inwardly facing surfaces of the innermost cladding capillaries, to form core boundary beads of the kind described herein with reference to structures S4 and S8. The rods 1835 can be selectively positioned on the inside of the large diameter capillary 1815 to be aligned with either or both of the longer or shorter core boundary veins. Of course, within practical limits, any number of rods 1835 may be attached to the inside, or indeed outside, of the large diameter capillary 1815. If attached on the outside of the large diameter capillary 1815, the rods 1235 may be aligned with the larger interstitial voids 1830.

The diameters of the rods are selected to provide the required bead size and may be of similar size or vary in size around the periphery of the large diameter capillary 1815.

In principle, rods 1835 may be attached to the inside or to the outside of the large diameter capillary 1815. Indeed, rods 1950 (see Figure 19) may in principle be attached to both the inside and the outside of the same region of the large diameter capillary, so that they form a relatively larger bead on the core boundary.

Figure 19 illustrates a similar pre-form stack suitable for forming a PBG fibre according to structure shown in Figure 15a.

The pre-form stack 1800 (or 1900) is arranged as described with reference to Figure 18 (or Figure 19) and is then over-clad with a further, relatively thick-walled capillary (see, for example, Figure 26), which is large enough to contain the stack and small enough to hold the capillaries and rods firmly in place. The entire over-clad stack is then heated and drawn into a so-called cane, during which time all the relatively large interstitial voids 1830 and any remaining voids between the glass rods 1825 and the cladding capillaries 1805, collapse due to surface tension. Then, the cane is, again, over-clad with a further, thick silica cladding tube (not shown) and is heated and drawn into optical fibre in a known way. If surface tension alone is insufficient to collapse any of the interstitial voids, a vacuum may be applied to the interstitial voids, either or both during drawing of the stack into a cane or the cane into the fibre, for example according to the process described in WO 00/49436 (The University of Bath).

Figure 20a is a photograph, taken by the present inventors through a microscope, of a rod fused to a large diameter capillary before the capillary is introduced into a pre-form stack. Whether the rod becomes a bead along a core boundary, for example as in structures S1, S4, S8 or S9, or a relatively more pronounced nodule protruding only from one side of a core boundary, for example as shown in Figures 15a-15c, can be controlled by the fibre drawing conditions. For example, hotter drawing conditions under lower tension permit a rod and boundary to fuse completely, thereby forming a bead. In contrast, a colder draw under higher tension prevents complete fusing of the rod and core boundary, leaving the rod as a nodule on the surface of the core boundary in a final fibre structure. Clearly, a nodule can be arranged to form on an inner or outer periphery of a core boundary, depending on whether the respective rod is positioned on an inner or outer periphery of a large diameter capillary of the pre-form stack. The properties of a final fibre structure are expected to vary with bead and/or nodule size and placement.

Figure 20b is an SEM image of a bead, which forms part of a PBG cladding structure according to an embodiment of the present invention. As shown, the bead has formed along a

relatively shorter vein of the cladding structure. The structure is a result of heating and drawing a preform containing the rod shown in Figure 20a. The drawing conditions included a heating temperature of about 2050°C, a draw speed of about $2ms^{-1}$ and a draw tension of about 240g. Clearly, the rod has fused completely with the capillary under these drawing conditions. It is expected that cooler and/or faster drawing conditions would lead to the formation of a nodule on the inner surface only of the capillary.

An alternative method of forming a pre-form stack 2100, which results in beads on shorter boundary veins only, is illustrated in Figure 21. Generally, the stack 2100 comprises the same arrangement of cladding capillaries 2105, and a large diameter capillary, as stack 1900. In this example, however, the larger interstitial voids 2130, which form between every other one of the innermost capillaries and the large diameter capillary 2115, are packed with a glass rod 2140 and two thin-walled capillaries 2145, which act to hold the glass rod 2140 in a central position in the void during drawing down into a cane. Unlike in stack 1900, the rods 2140 and capillaries 2145 are not fused to the large diameter capillary 2115 before it is introduced to the stack 2100. Rather, they are introduced into the stack during assembly thereof. When the stack 2100 is heated and drawn down, the rods 2140 form beads on the shorter boundary veins and the thin-walled capillaries collapse entirely – if necessary with the application of a vacuum - adding an insignificant amount of material to the overall structure.

The pre-form stack of Figure 21 may be modified slightly as shown in Figure 22, whereby the thin-walled capillaries 2145, on either side of the glass rods 2140, are replaced by additional glass rods 2250. The effect is that, when the stack is drawn down to a fibre, the three glass rods in each void increase the overall thickness of the associated boundary vein, whereby thicker boundary veins are created, as in the structures in Figure 15d.

Thicker boundary veins may alternatively be formed in accordance with the pre-form stack 2300 shown in the diagram in Figure 23. While the cladding capillaries are arranged in the same way as in previously described stacks, the inner region of the stack 2300 is formed using two concentric, slightly different sized, large diameter capillaries, 2315 and 2316. The larger of the large diameter capillaries supports the cladding capillaries, while the smaller of the large diameter capillaries fits within the larger one. The smaller large diameter capillary is sufficiently small that relatively small rods 2340 and capillaries 2345 can fit in the space between the larger and smaller large diameter capillaries.

When the stack 2300 is heated and drawn down into a cane and a fibre, the rods 2340 become thicker boundary veins and the capillaries 2345 collapse to form part of the thinner boundary veins.

Thicker boundary veins may alternatively be produced by pre-profiling a large diameter capillary 2415, for example by using an etching process. First, as shown in Figure 24a, a masking agent 2410 is applied to a large diameter capillary 2415 in positions which correspond to required regions of increased thickness in a final fibre structure. The masking agent 2410 is one which inhibits etching by HF, for example a polymer-based photo-resist or a noble metal-based material. According to Figure 24b, the capillary is subjected to a flow of HF in an MCVD lathe (in a known manner), whereby the unmasked capillary surfaces 2420 are etched away to the degree required. Finally, the mask is removed and, as shown in Figure 24c, the capillary 2415 is used in a capillary stack 2400, in which the thicker regions of the capillary 2415 are aligned with the regions of the stack where thicker boundary veins are required. Of course, masking and etching may selectively be applied to inner and/or outer surfaces and regions of the capillary depending of the required final form of the capillary.

Alternatively, a core boundary may comprise a predominantly thick-walled core boundary (not shown) around which relatively short regions of material have been etched away. This is in contrast to the thin-walled boundary with a number of relatively short thicker regions. A similar, predominantly thick-walled core boundary may be made in a different manner by heating and 'pinching' regions of a large diameter capillary prior to it being inserted into a capillary stack. Pinched regions of the capillary would form relatively short, thinner regions in a final core boundary, and addition of several appropriately-placed pinches may be used to fine-tune the resulting fibre structure. The capillary could be pinched between two elongate tungsten blades, one on the inside of the capillary and the other aligned with the first on the outside, for example, while the capillary is hot enough to be deformed.

An alternative method for forming a capillary stack 2500, which does not require a large diameter capillary, is illustrated in Figure 25. A large diameter capillary is omitted and an insert 2515 is used instead; for example made of graphite, platinum, tungsten or a ceramic material, which has a higher melting point than silica glass and, preferably, a higher coefficient of thermal expansion.

The insert 2515 is shaped, by having detents, to support cladding capillaries and rods and also to support additional glass rods 2510, which eventually become pronounced beads 150.

The stack 2500, including the insert 2515, is heated to allow the capillaries and rods to fuse into a pre-form. The pre-form is then allowed to cool and the insert 2515 is removed. It will be apparent that, at this point, the inwardly-facing walls of the innermost capillaries take on the general shape of the insert 2515. An advantage of using an insert material having a higher coefficient of thermal expansion than silica is that, when the pre-form and insert are heated, the insert expands and, relatively-speaking, increases the area of the central region in which the insert is located. When permitted to cool down again, the insert shrinks back down to its original size and the silica solidifies before shrinking fully back down, leaving an inner region that is larger than the insert. The insert 2515, which, as a result, is loose-fitting in the central region, may then be removed readily from the pre-form with reduced risk of damaging or contaminating the pre-form 2500. The resulting pre-form is then heated and drawn in the usual way, in one or more drawing steps.

A further alternative way to form the fibre is by using a process similar to that described in PCT/GB00/01249, wherein the cladding capillaries and rods, and additional capillaries and/or rods for shaping the boundary, are supported by truncated capillaries at either end of the stack. The stack may be drawn to an optical fibre in the normal way, and the parts of the fibre incorporating the truncated capillary material may be discarded. In principle, truncated capillaries may also be used to support the stack part way along its length.

The diagram in Figure 26 illustrates a small portion of an outer region of a pre-form stack 2600 made from circular cross section capillaries 2620. In this embodiment, the entire stack is contained in a large circular cross section capillary tube 2670, having a generally circular bore, which is large enough to receive the entire assembled stack as a sliding fit. As shown, interstitial voids 2675 form between the edges of the stack and the internal surface of the large capillary. It has been found beneficial to pack these interstitial voids with circular cross section packing rods 2680, having various sizes selected to support all cladding capillaries in their appropriate positions within the large capillary. These rods melt and fuse with the large circular capillary to form a homogenous outer layer of glass that surrounds the microstructured inner region.

Figure 27 is a diagram of a transmission system 2700 comprising an optical transmitter 2710, an optical receiver 2720 and an optical fibre 2730 between the transmitter and receiver. The optical fibre 2730 comprises along at least a part of its length an optical fibre according to an embodiment of the present invention. Other components or systems, for

example to compensate for dispersion and loss, would typically be included in the system but are not shown in Figure 27 for the sake of convenience only.

The skilled person will appreciate that the various structures described above may be manufactured using the described manufacturing process or a prior art processes, which is adapted to modify the core boundary. For example, rather than using a stacking and drawing approach to manufacture, a pre-form may be made using a known extrusion process and then that pre-form may be drawn into an optical fibre in the normal way.

In addition, the skilled person will appreciate that while the examples provided above relate generally to air-core-guiding PBG fibre structures, comprising triangular cladding arrays, the present invention is in no way limited to such structures. For example, the invention could relate equally to square lattice structures, structures that are not close-packed, or structures with coaxial claddings. Indeed, the structures need not guide light by band-gap guidance. In general, the inventors propose that given a core region that supports guided modes, the form of the boundary at the interface between the core region and the cladding structure will have a significant impact on the characteristics of the waveguide, as described herein.

The skilled person will also appreciate that the structures described herein fit on a continuum comprising a huge number of different structures, for example having different combinations of core defect size, boundary node size, boundary vein thickness and, in general, boundary and cladding form. Clearly, it would be impractical to illustrate each and every variant of waveguide structure herein. As such, the skilled person will accept that the present invention is limited in scope only by the present claims

CLAIMS

1. An elongate waveguide for guiding light comprising:

a core, comprising an elongate region of relatively low refractive index;

a microstructured region around the core comprising elongate regions of relatively low refractive index interspersed with elongate regions of relatively high refractive index; and

a boundary at the interface between the core and the microstructured region, the boundary comprising, in the transverse cross-section, a region of relatively high refractive index, which is connected to the microstructured region at a plurality of nodes, characterised by at least one relatively enlarged region around the boundary (and excluding a boundary having twelve nodes and six enlarged regions substantially at a mid-point between six pairs of relatively more-widely-spaced apart neighbouring nodes).

2. A waveguide according to any one of the preceding claims, wherein there are plural enlarged regions around the boundary.

3. A waveguide according to either preceding claim, wherein the or at least one enlarged region is positioned between neighbouring nodes.

4. A waveguide according to any one of the preceding claims, wherein there are six enlarged regions around the boundary.

5. A waveguide according to any one of the preceding claims, wherein there are more than six enlarged regions around the boundary.

6. A waveguide according to any one of the preceding claims, wherein there are twelve or more enlarged regions around the boundary.

7. A waveguide according to any one of the preceding claims, wherein the core boundary comprises eighteen nodes.

8. A waveguide according to any one of the preceding claims, wherein there are enlarged regions between six or more pairs of neighbouring nodes.

9. A waveguide according to any one of the preceding claims, wherein the boundary has at least enlarged regions between twelve pairs of neighbouring nodes.

10. A waveguide according to any one of the preceding claims, wherein there is only one enlarged region between any pair of neighbouring nodes.

11. A waveguide according to any one of claims 1 to 9, wherein there are plural enlarged regions between at least one pair of neighbouring nodes.

12. A waveguide according to any one of the preceding claims, wherein there are plural enlarged regions that are substantially equi-spaced around the boundary.

13. A waveguide according to any one of claims 1 to 11, wherein there are plural groups of two or more enlarged regions and the groups are substantially equi-spaced around the boundary.

14. A waveguide according to any one of the preceding claims, wherein the nodes around the boundary are connected by relatively high refractive index veins.

15. A waveguide according to claim 14, wherein a plurality of enlarged regions are positioned along veins and spaced apart from any nodes.

16. A waveguide according to claim 14, wherein an enlarged region comprises a relatively thick vein, compared to the thickness of at least one other vein, extending between a pair of neighbouring nodes.

17. A waveguide according to any one of the preceding claims, wherein the boundary comprises at least one ridged region, characterised by plural enlarged regions in relatively close proximity.

18. A waveguide according to claim 17, wherein there are plural ridged regions around the boundary

19. A waveguide according to claim 17, wherein a significant portion of the boundary is ridged.

20. A waveguide according to any one of the preceding claims, wherein at least one enlarged region is located on an outer periphery of the boundary.

21. A waveguide according to any one of the preceding claims, wherein at least one enlarged region is located on an inner periphery of the boundary.

22. A waveguide according to any one of the preceding claims, wherein there is at least one enlarged region on both the inner and outer periphery of the boundary.

23. A waveguide according to any one of the preceding claims, wherein the microstructured region, in the plane cross section, comprises a substantially periodic array of relatively low refractive index regions, being separated from one another by relatively high refractive index regions, the array having a characteristic primitive unit cell and a pitch Λ.

24. A waveguide according to any one of the preceding claims, wherein the microstructured region comprises a substantially periodic, triangular array of relatively low refractive index regions.

25. A waveguide according to claim 24, wherein the core is a seven cell defect.

26. A waveguide according to claim 24, wherein the core is a nineteen cell core defect.

27. A waveguide according to any one of the preceding claims, wherein at least some of the relatively low refractive index regions are voids are under vacuum or are filled with air or another gas.

28. A waveguide according to any one of the preceding claims, wherein at least some of the relatively high refractive index regions comprise silica glass.

29. A waveguide according to any one of the preceding claims, wherein at least some of the boundary veins are substantially straight.

30. A waveguide according to any one of the preceding claims, wherein the microstructured region comprises a photonic band-gap structure.

31. A waveguide according to claim 30, wherein at least some of the enlarged regions deviate from the form of the photonic band-gap structure.

32. A waveguide according to claim 31, wherein an enlarged region is coincident with a node such that the node appears to have an uncharacteristic form relative to the photonic band-gap cladding.

33. A waveguide according to any one of the preceding claims, wherein the proportion by volume of relatively low refractive index regions in the microstructured region is greater than 75%.

34. A waveguide according to any one of the preceding claims, which supports a mode in which greater than 95% of the mode power in the waveguide is in relatively low refractive index regions.

35. A waveguide according to any one of the preceding claims, which supports a mode having a mode profile that closely resembles the fundamental mode of a standard, single mode optical fibre.

36. A waveguide according to claim 35, wherein said mode supports a maximum amount of the mode power in relatively low refractive index regions compared with other modes that are supported by the waveguide.

37. A waveguide according to any one of the preceding claims, which supports a core-guided, non-degenerate mode.

38. A waveguide according to claim 37, wherein said mode is the lowest loss mode of the waveguide.

39. A waveguide according to claim 35, wherein said mode is the lowest loss mode of the waveguide.

40. A waveguide according to any one of the preceding claims, which supports plural core-guided modes.

41. A waveguide according to any one of claims 24 to 40, having an operating wavelength, wherein the pitch of the microstructured region is greater than the operating wavelength.

42. An optical fibre comprising a waveguide according to any one of the preceding claims.

43. A transmission line for carrying data between a transmitter and a receiver, the transmission line including along at least part of its length a fibre according to claim 42.

44. A preform for a microstructured optical fibre waveguide, comprising a stack of parallel, first elongate elements supported, in the plane cross section, around an inner region, which is to become a relatively low refractive index core region when the preform is drawn into a fibre, the preform further comprising second elongate elements, also supported or situated around the inner region, said second elements being arranged to generate a core boundary, at the interface between the photonic band-gap cladding and the core, when the preform is drawn into fibre, the arrangement of second elements being such that the core boundary comprises at least one relatively enlarged region when the preform is drawn into fibre.

45. A preform according to claim 44, further comprising a third elongate element for supporting the first and second elongate elements around the inner region.

46. A preform according to claim 45, wherein the third elongate element is a solid member.

47. A preform according to claim 45, wherein the third elongate elements has a bore.

48. A preform according to claim 46 or claim 47, wherein at least some of the second elongate elements are situated in interstitial regions that form between the first elongate elements and the third elongate element.

49. A preform according to claim 46 or claim 47, wherein the third elongate element has at least one elongate detent around its periphery and one or more of the second elongate elements are situated in the detent or detents.

50. A preform according to claim 47, wherein at least some second elongate elements are attached to an outer periphery of the third elongate element.

51. A preform according to claim 47, wherein at least some second elongate elements are attached to an inner periphery of the third elongate element.

52. A preform according to claim 50 or claim 51, wherein said second elongate elements are fused to the third elongate element.

53. A preform according to claim 47, wherein the third elongate is pre-profiled, in the transverse cross section, to have around its periphery enlarged regions that constitute the second elongate elements.

54. A preform according to claim 45, wherein the third elongate element comprises an inner capillary within the bore of an inside an outer capillary, and at least some second elongate elements are situated in a region that is formed between the inner capillary and the outer capillary.

55. A preform according to any one of claims 44 to 54, wherein said first elongate elements are arranged, on a macro scale, to become a photonic band-gap cladding structure when the preform is drawn into a fibre.

56. A preform according to claim 55, , wherein the arrangement of second elongate elements deviates from the arrangement of first elongate elements required to form the photonic band-gap cladding structure.

57. A preform according to any one of claims 44 to 56, wherein at least some of the second elongate elements comprise solid rods.

58. A preform according to any one of claims 44 to 57, wherein at least some of the second elongate elements comprise capillaries.

59. A preform according to any one of claims 44 to 58, wherein at least some of the first elements have a circular cross section.

60. A preform according to claim 59, wherein at least some of said circular first elements are capillaries.

61. A preform according to claim 60, wherein said capillaries are arranged in a triangular array.

62. A preform according to claim 61, wherein other first elongate elements are solid rods that are situated in interstitial regions between the capillaries.

63. An optical fibre made from a preform as claimed in any one claims 44 to 62.

64. A method of forming a photonic band-gap fibre, comprising the steps of forming a preform according to any one of claims 40 to58, and heating and drawing the preform, in one or more stages, into the fibre.

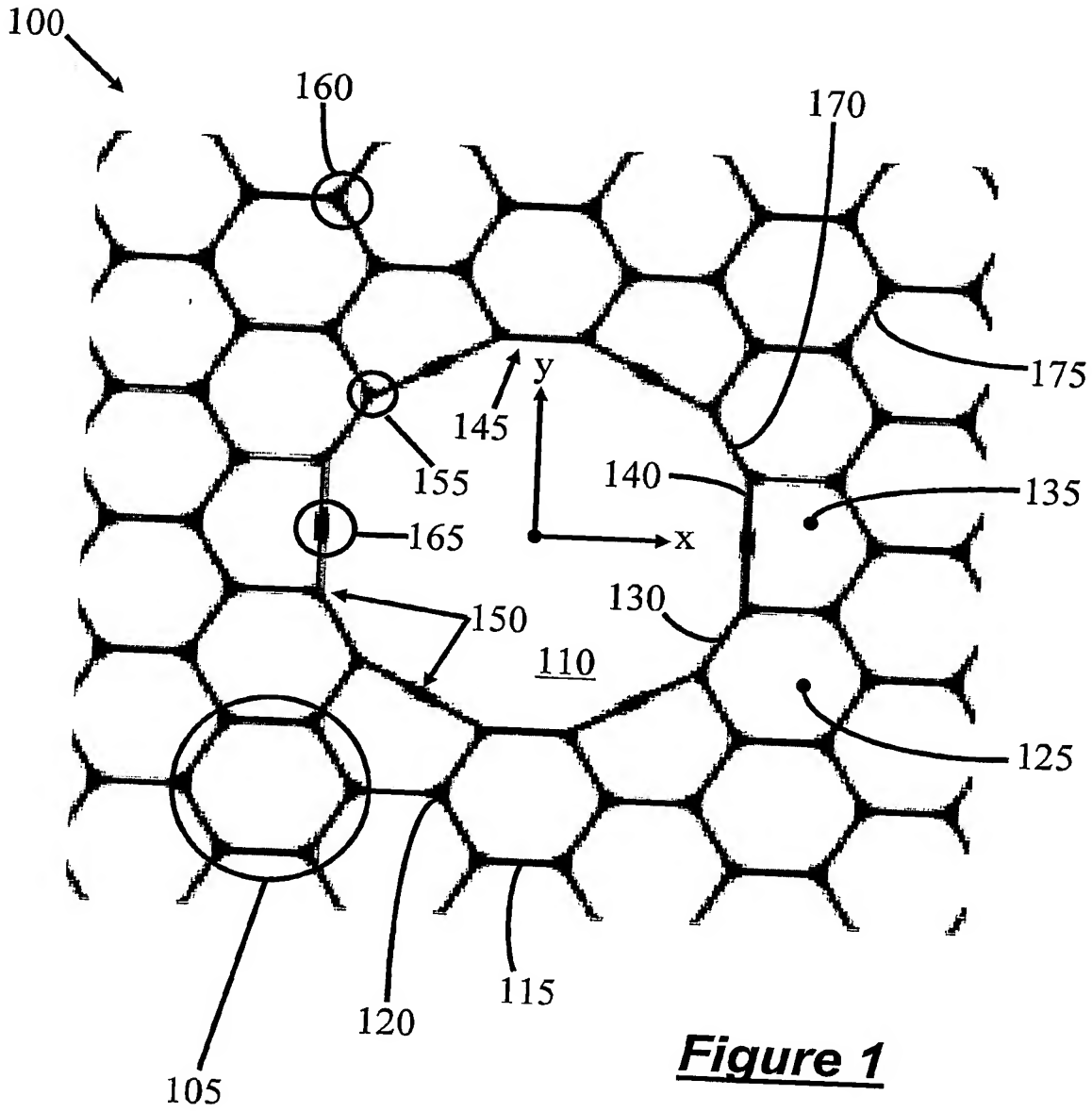
100
160
170
175
y
145
155
140
135
165
x
150
130
110
125
115
120
105

Figure 1

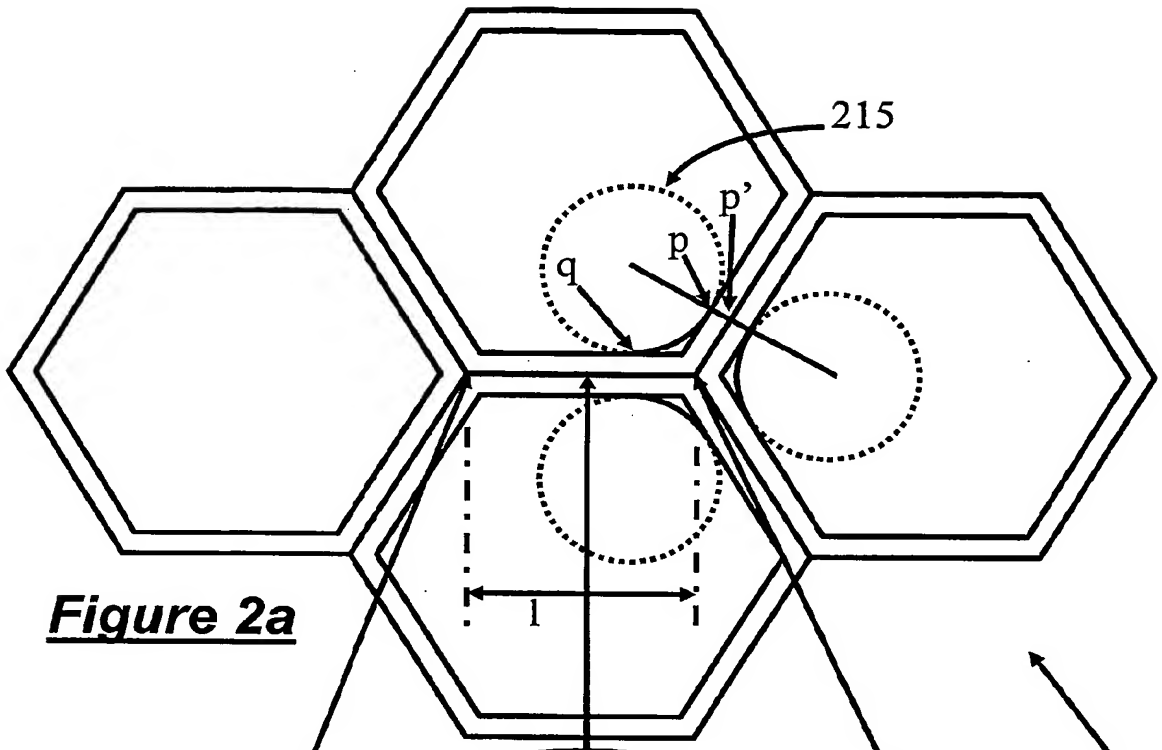

Figure 2a

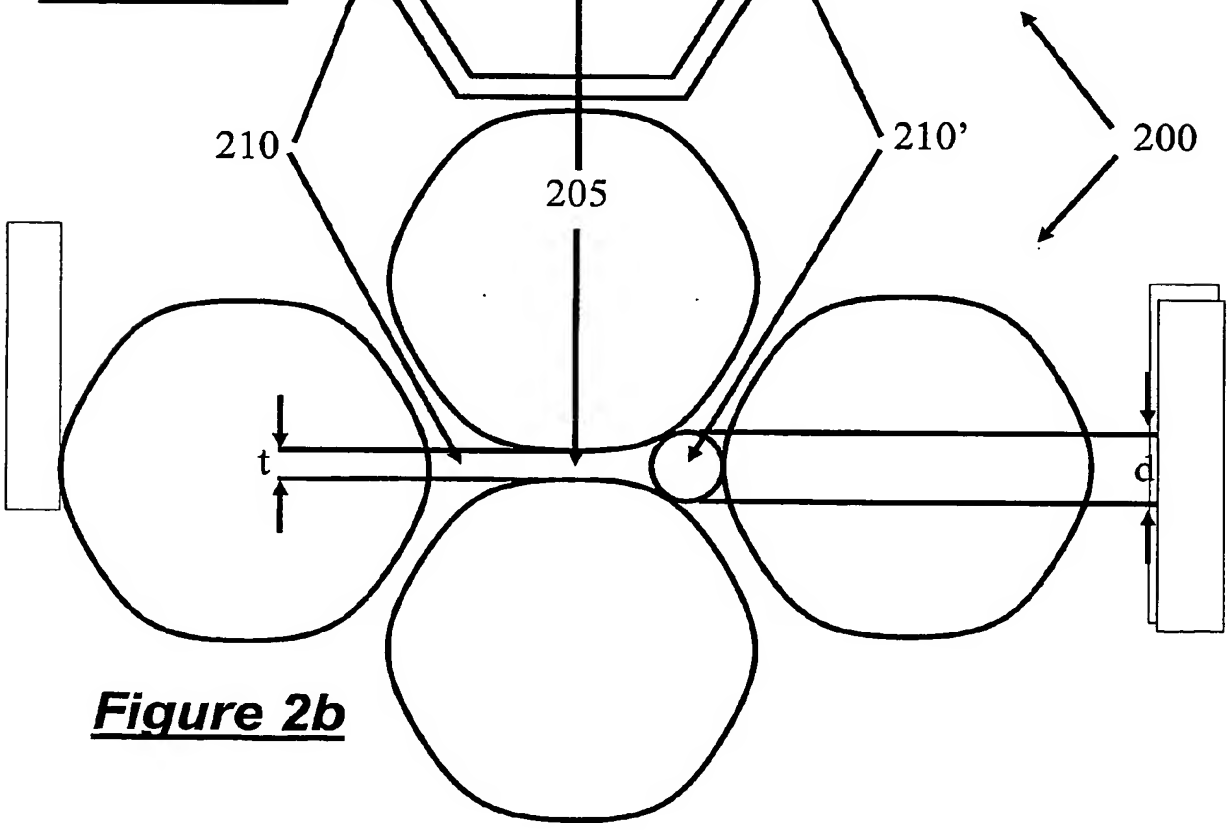

Figure 2b

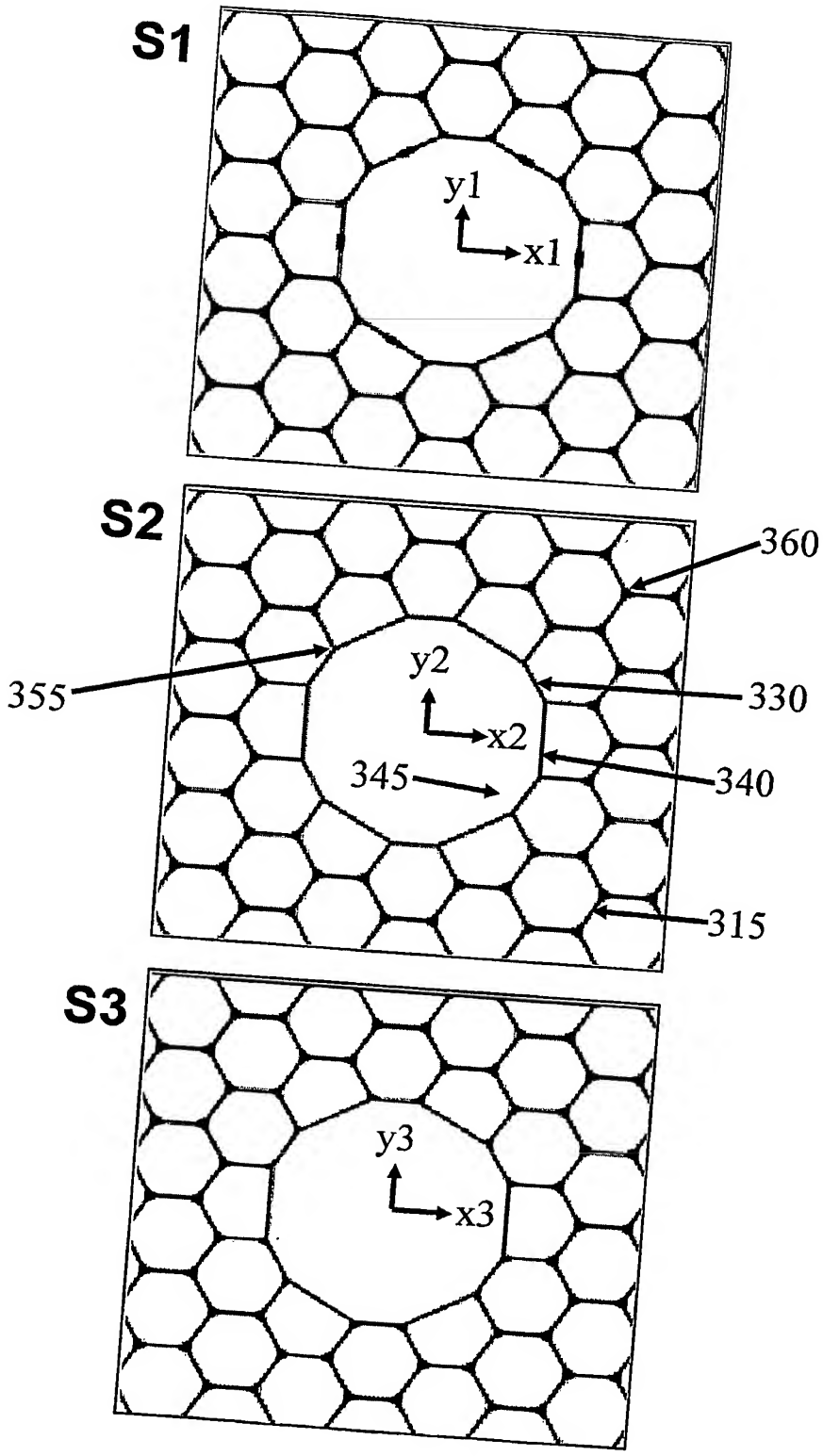

Figure 3

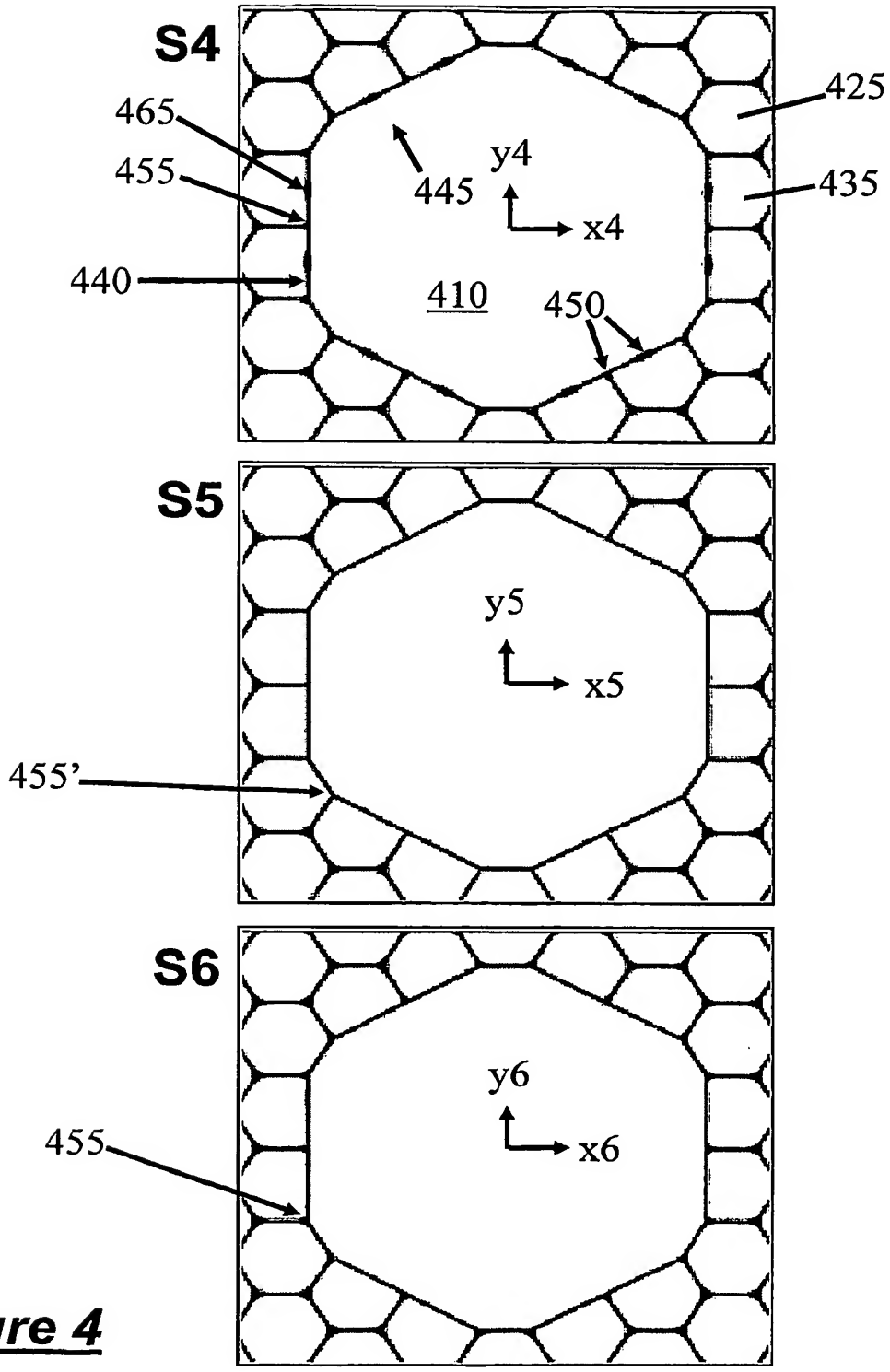

Figure 4

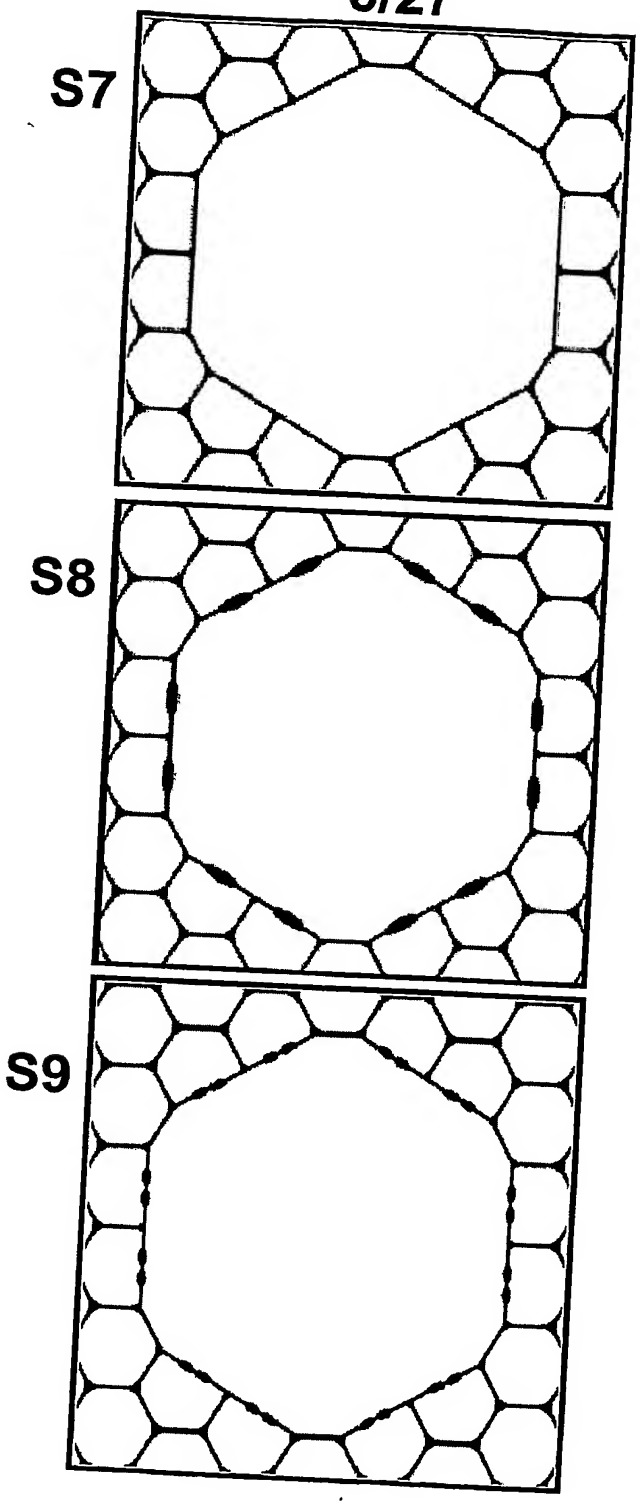

Figure 5

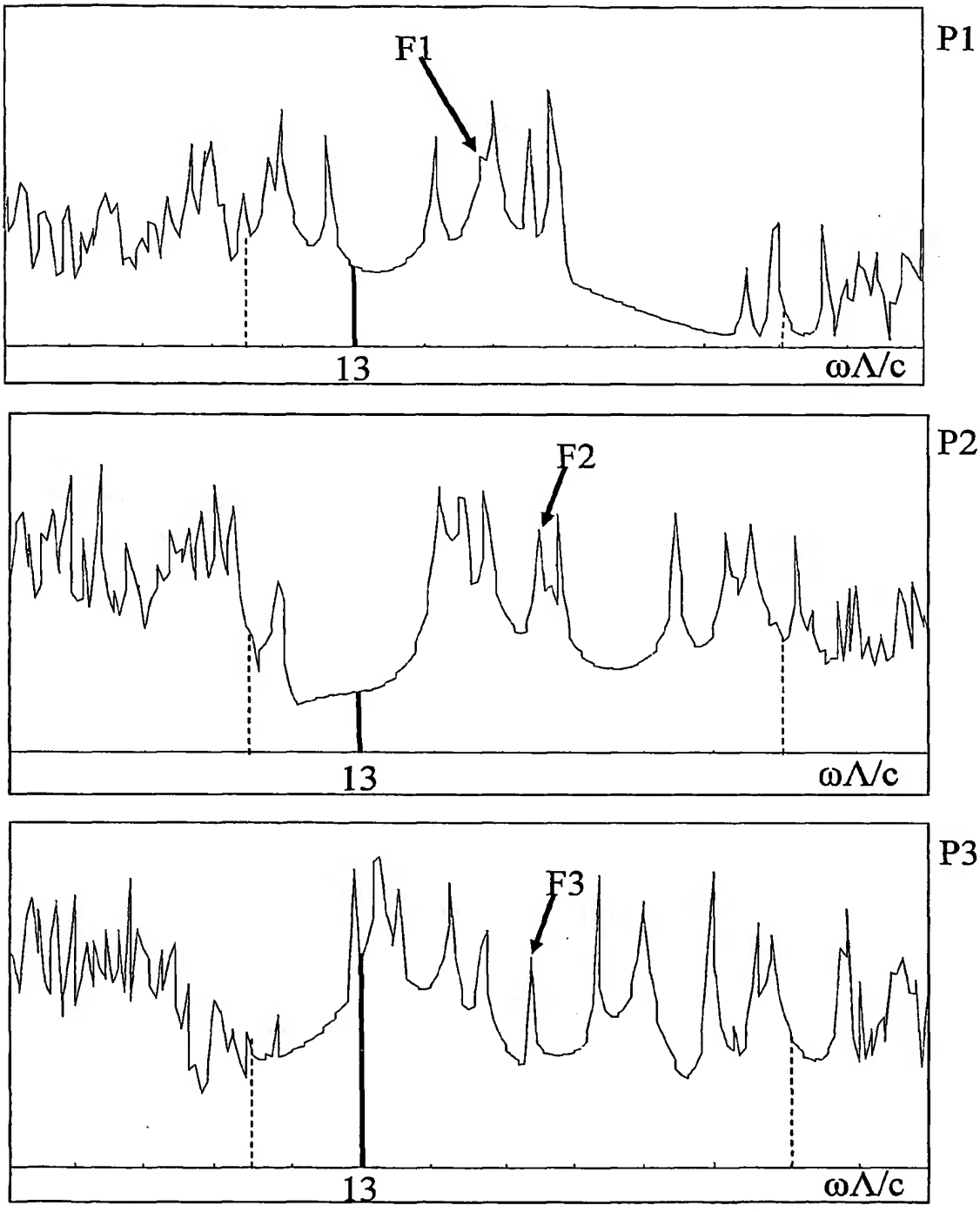

Figure 6

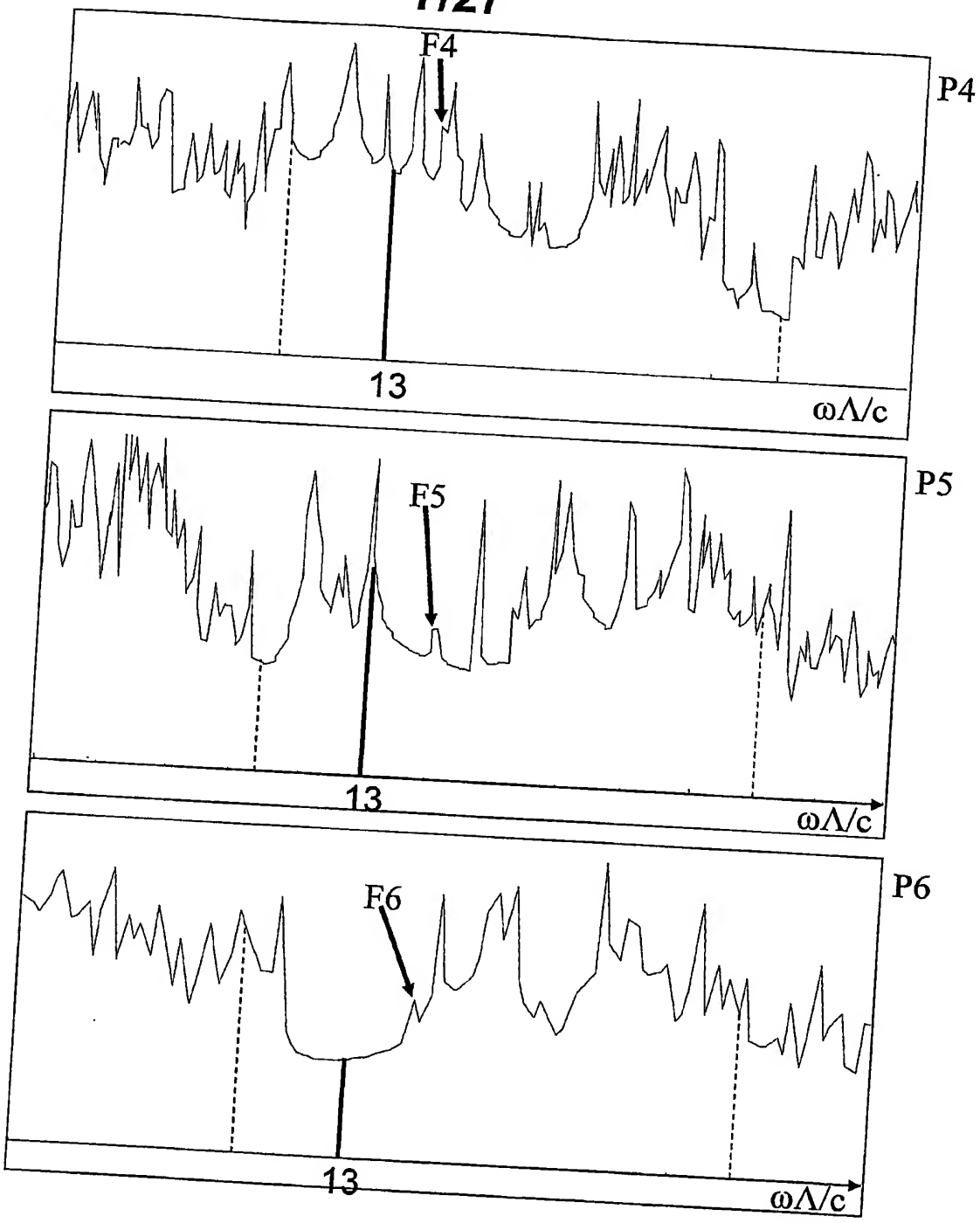

Figure 7

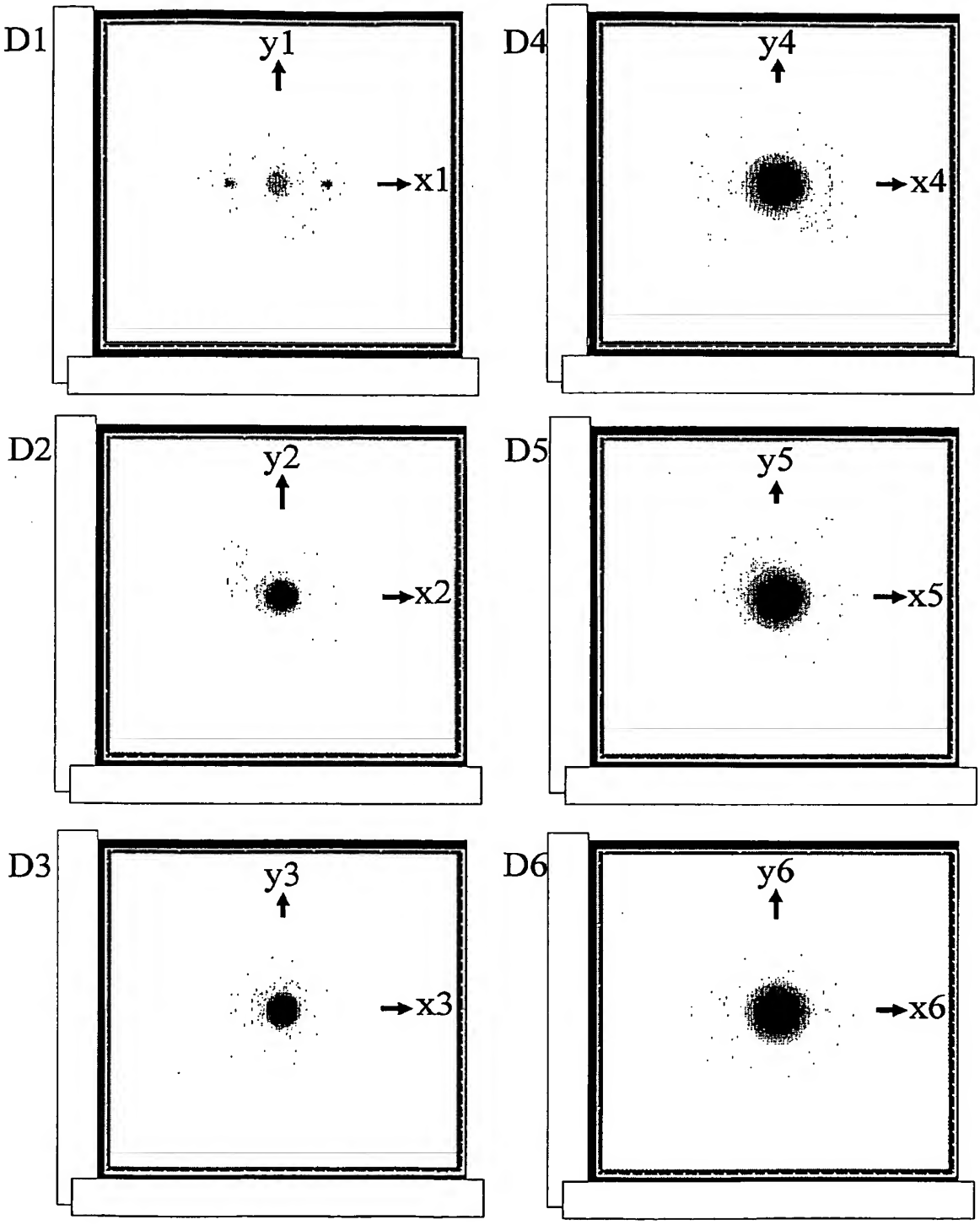

Figure 8

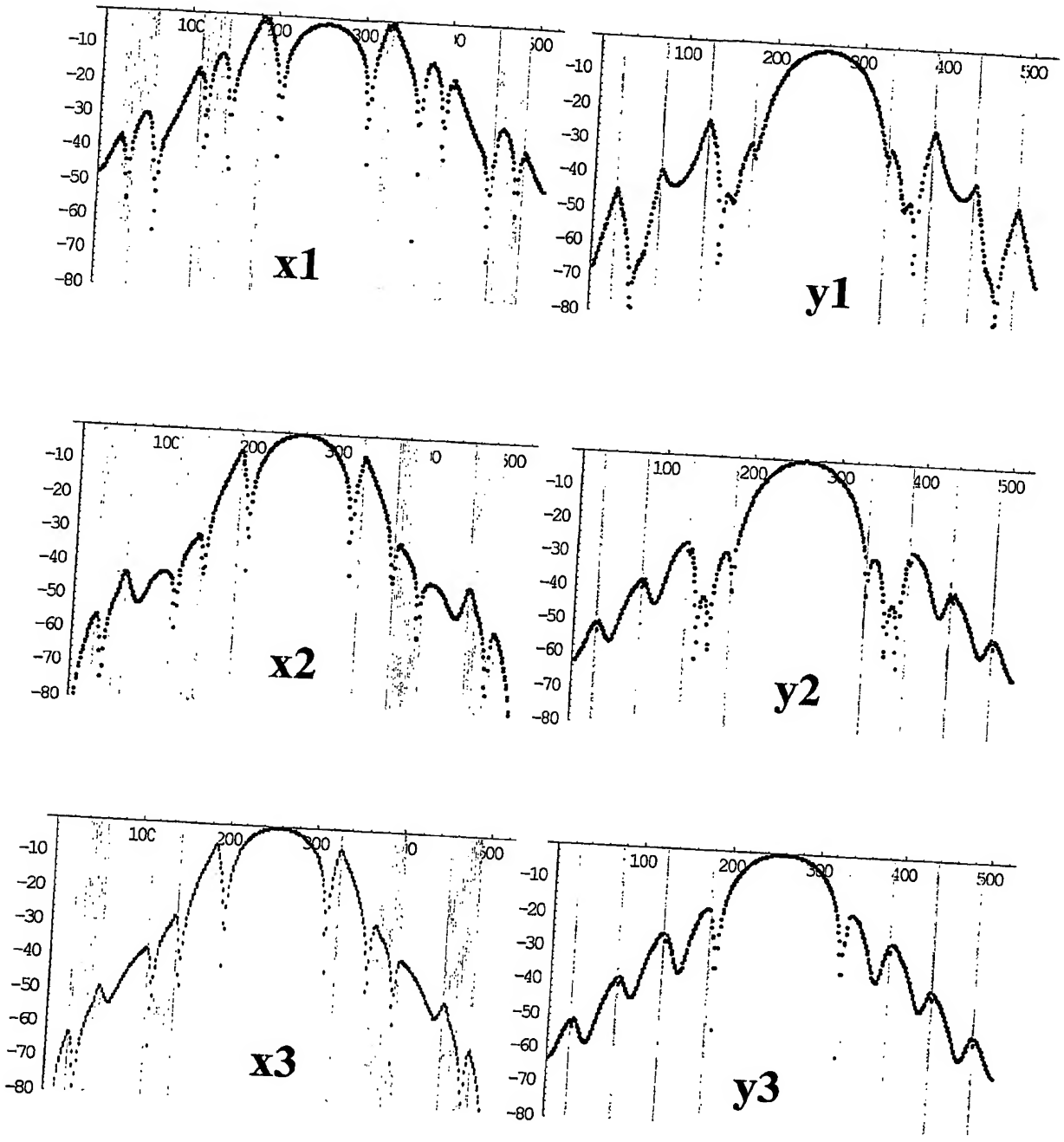

Figure 9

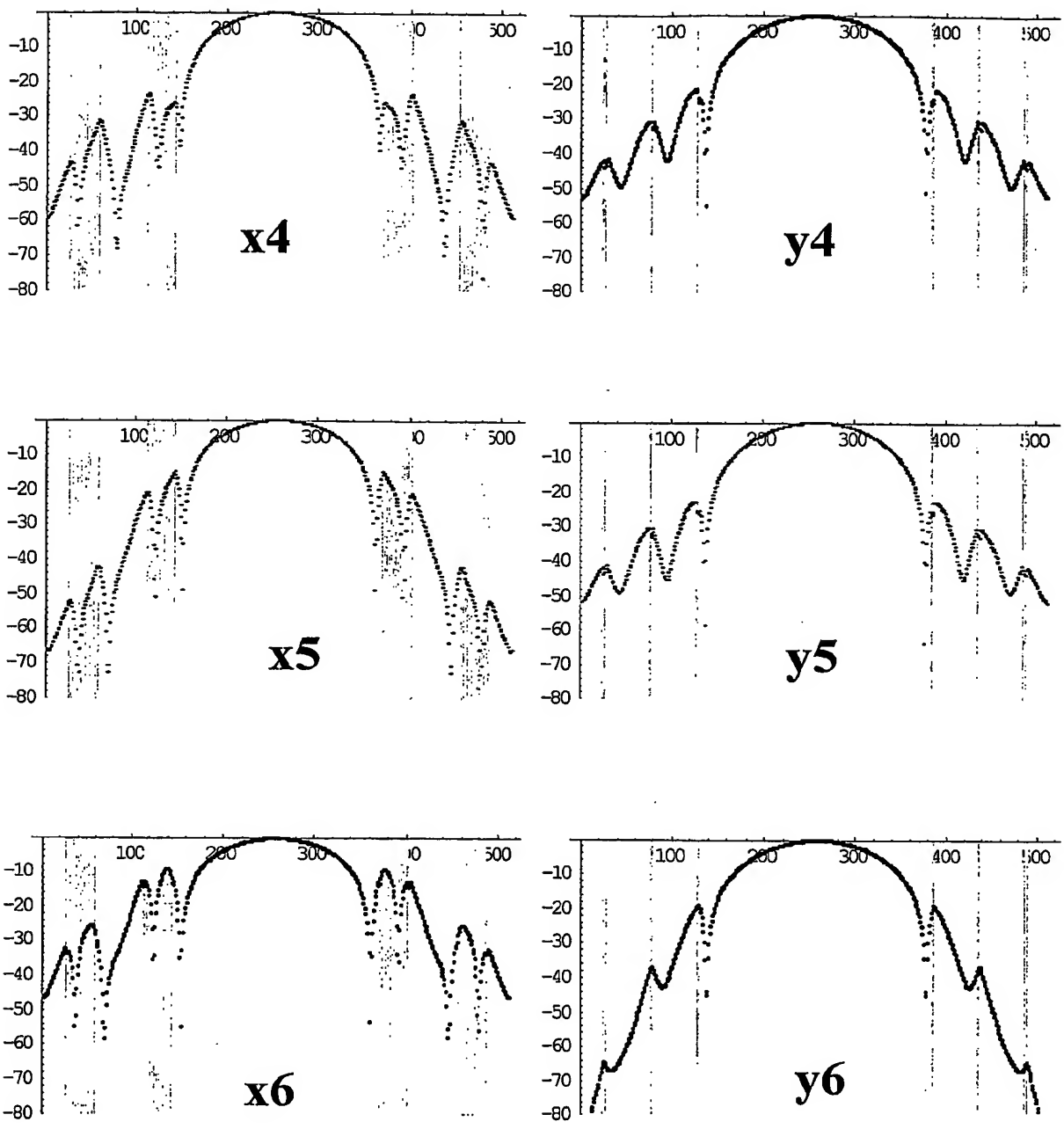

Figure 10

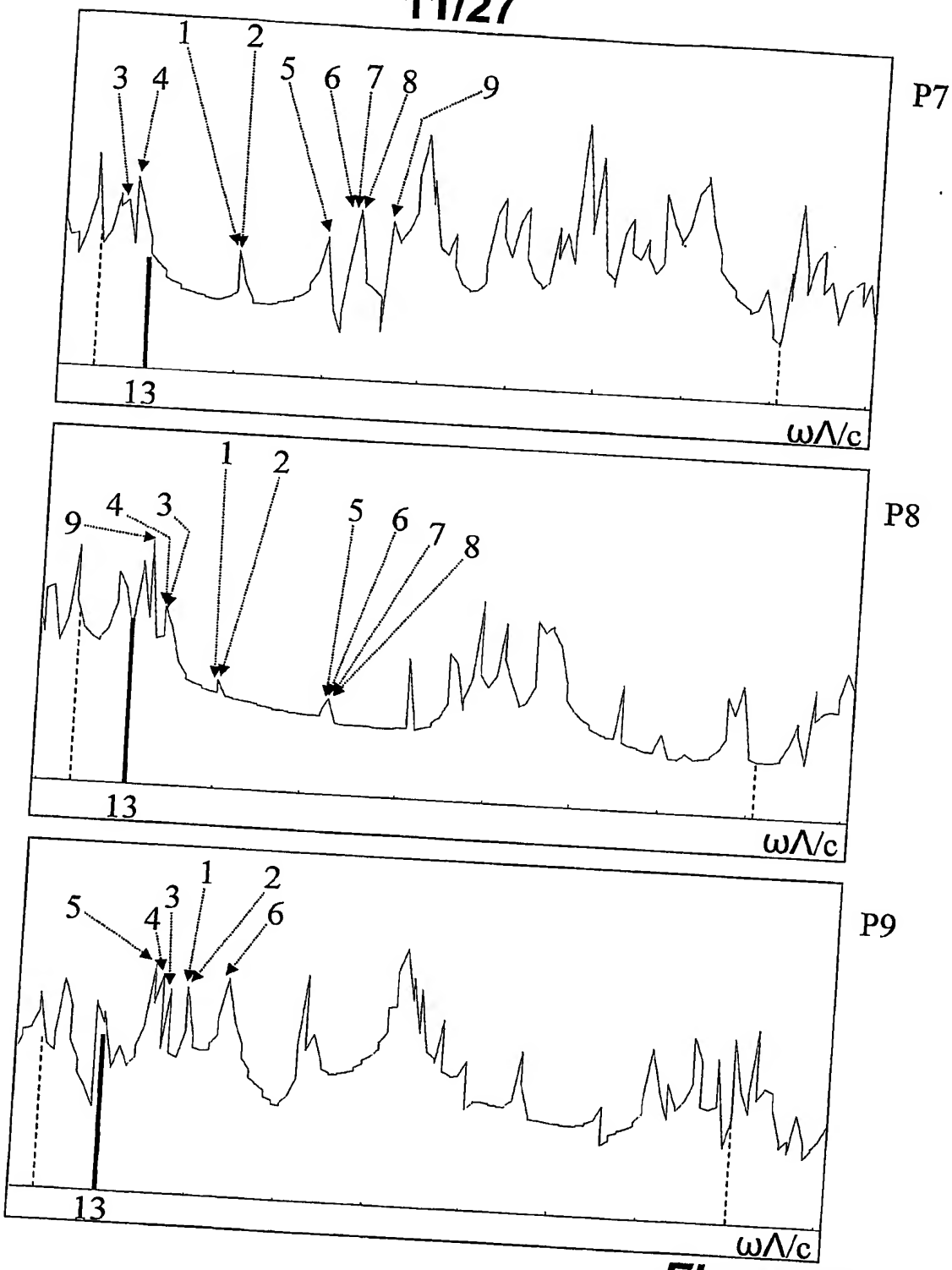

Figure 11

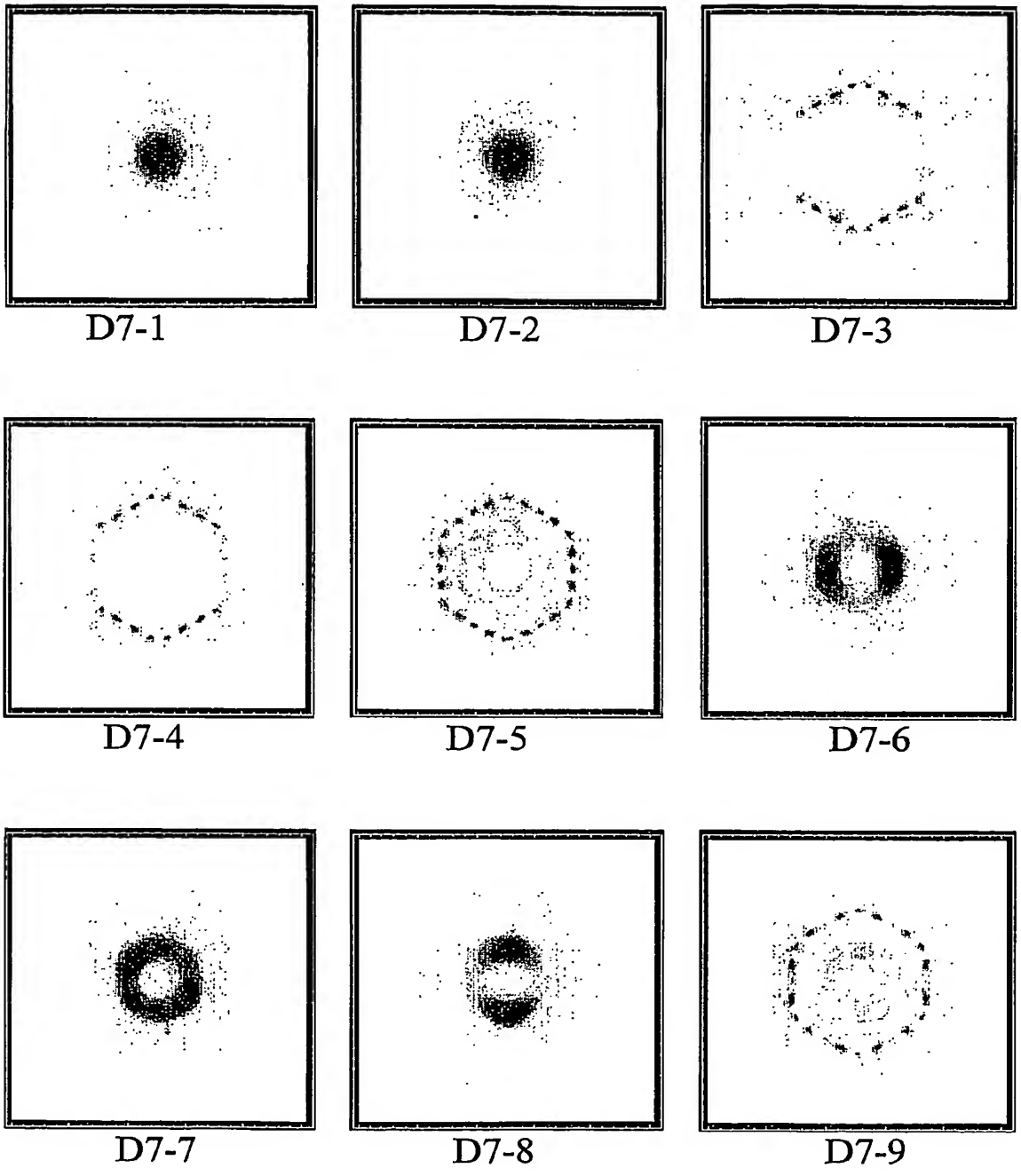

Figure 12

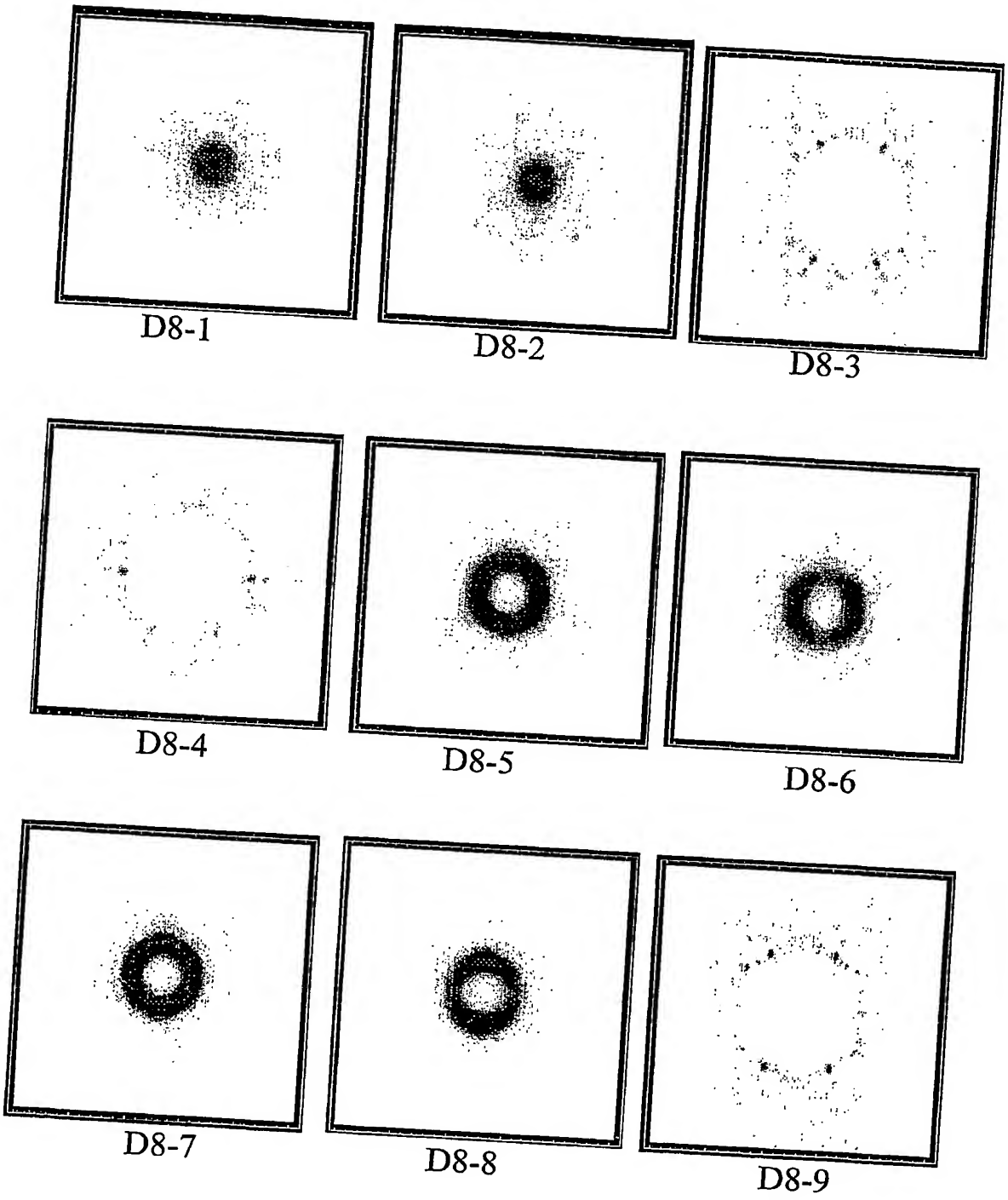

Figure 13

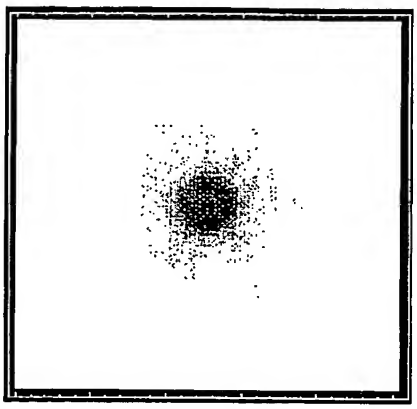

D9-1

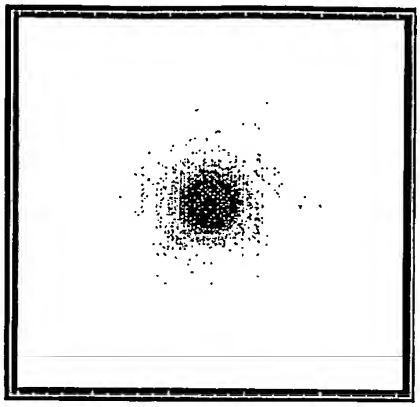

D9-2

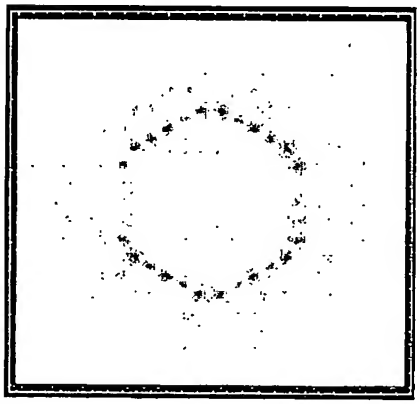

D9-3

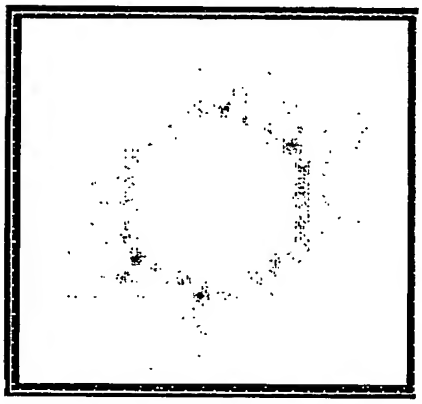

D9-4

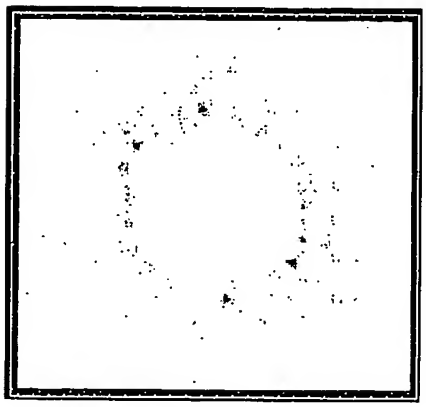

D9-5

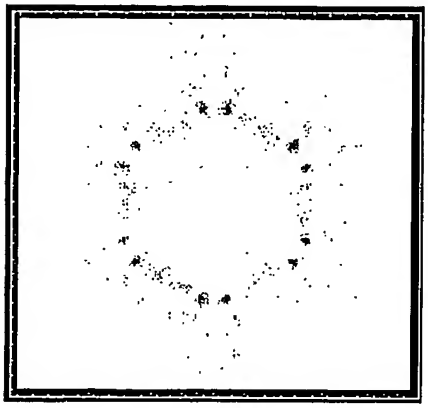

D9-5

Figure 14

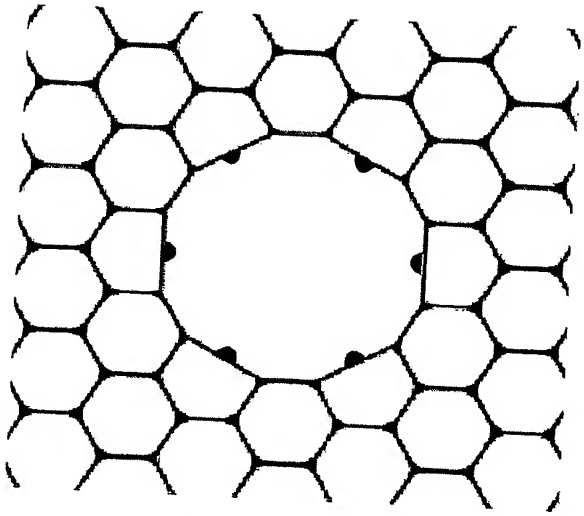

Figure 15a

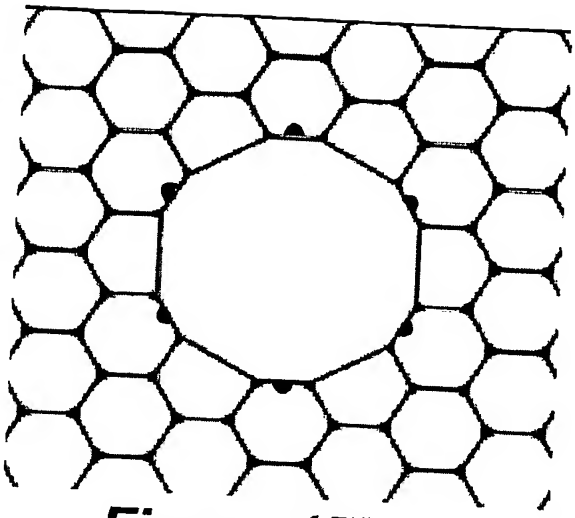

Figure 15b

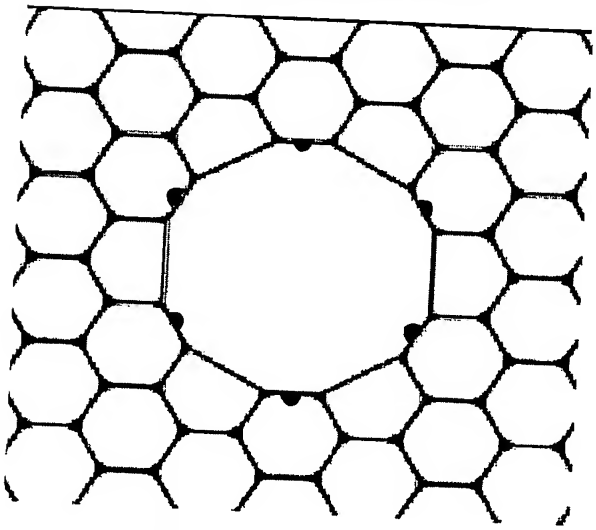

Figure 15c

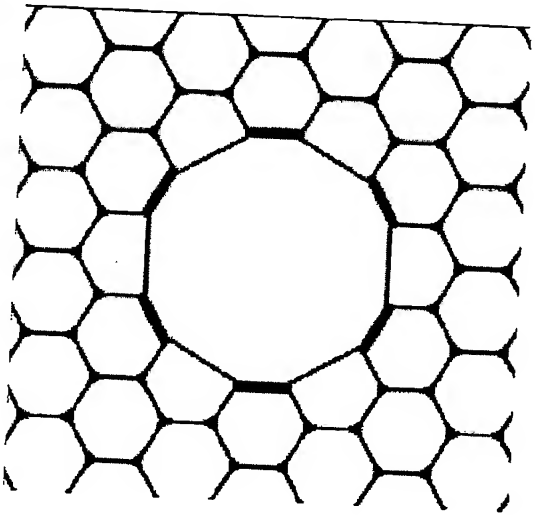

Figure 15d

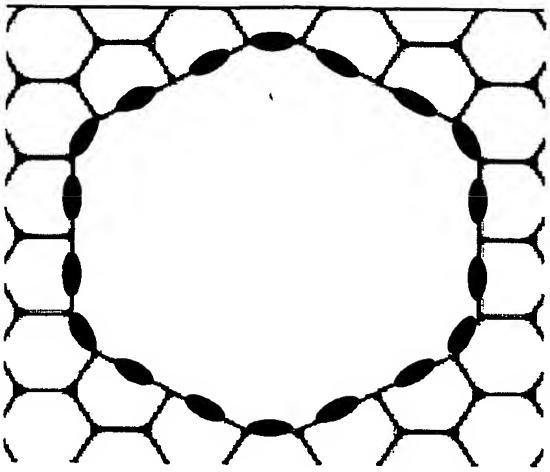

Figure 16a

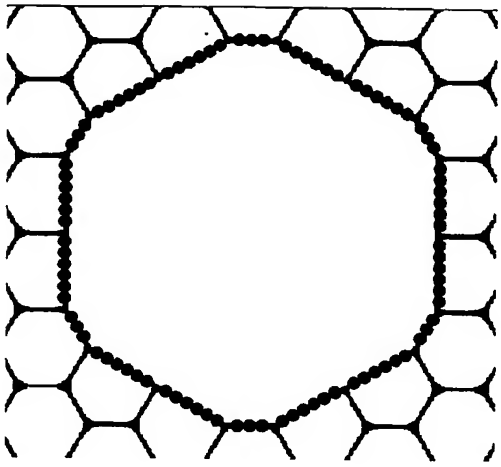

Figure 16b

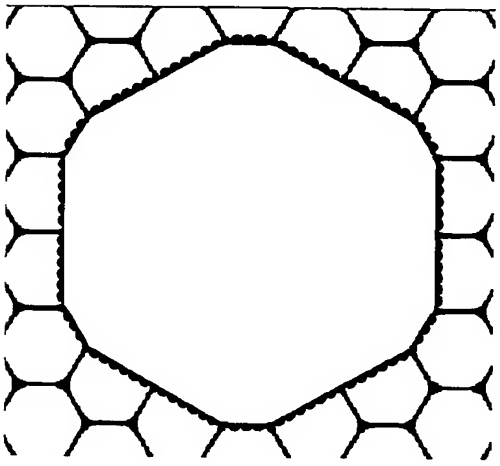

Figure 16c

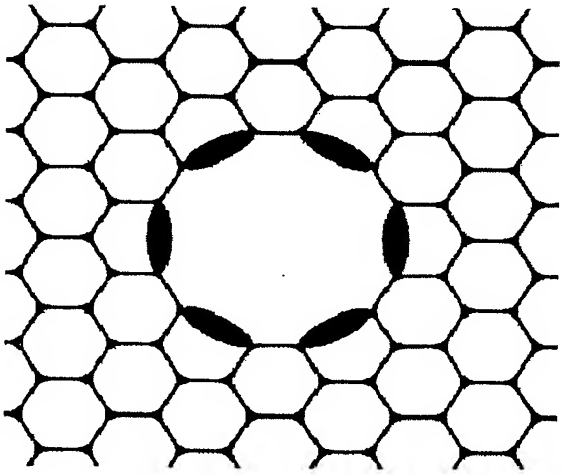

Figure 16d

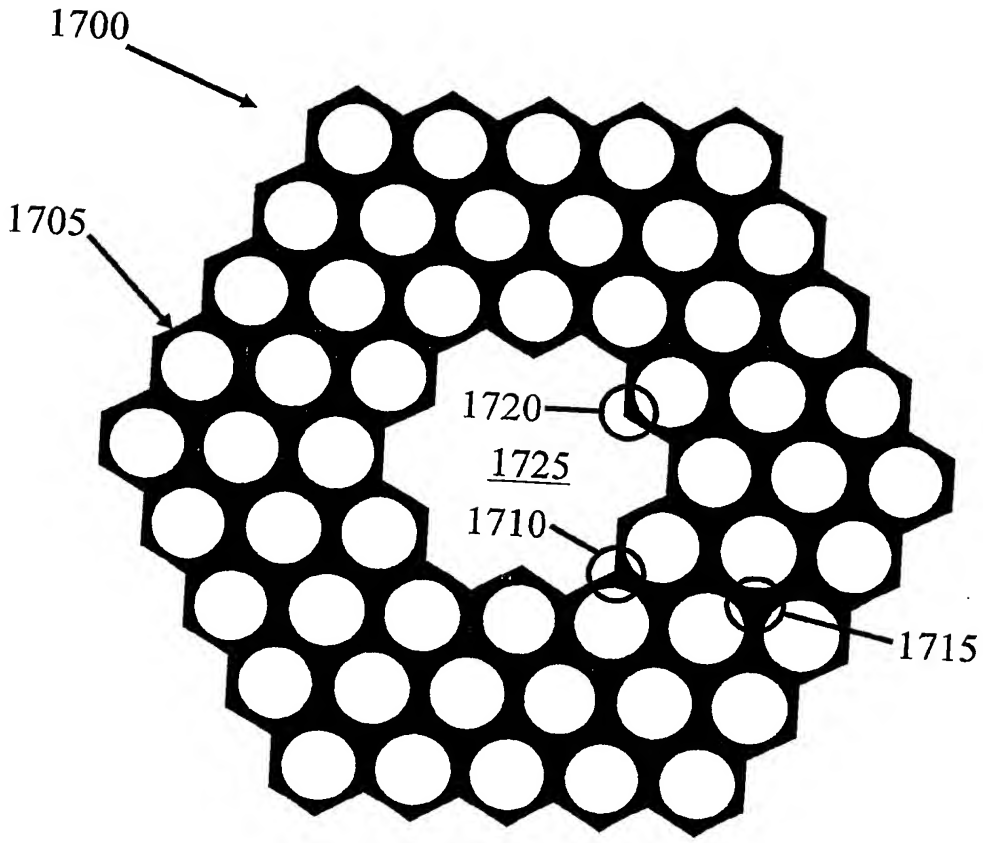

Figure 17

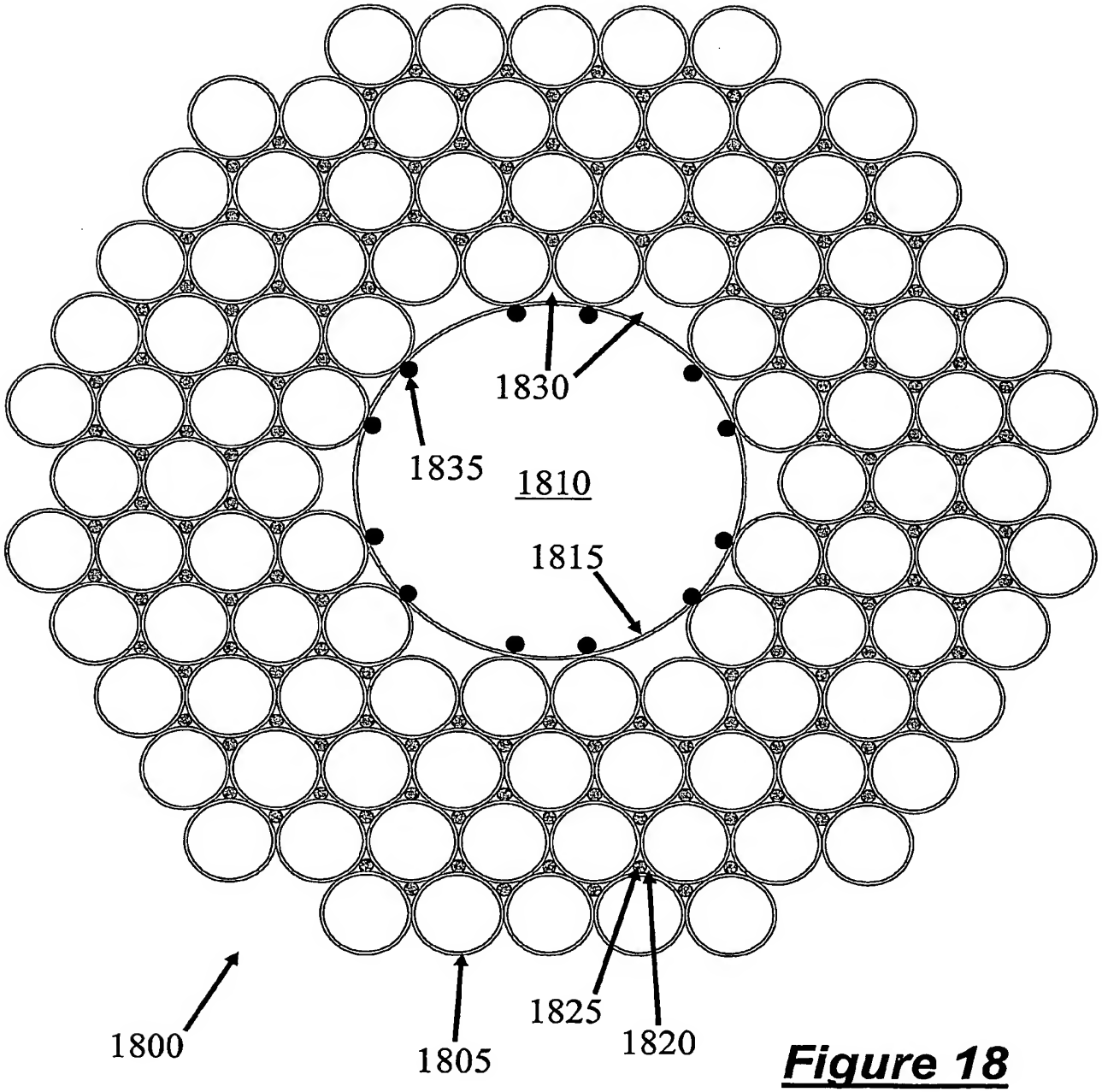

Figure 18

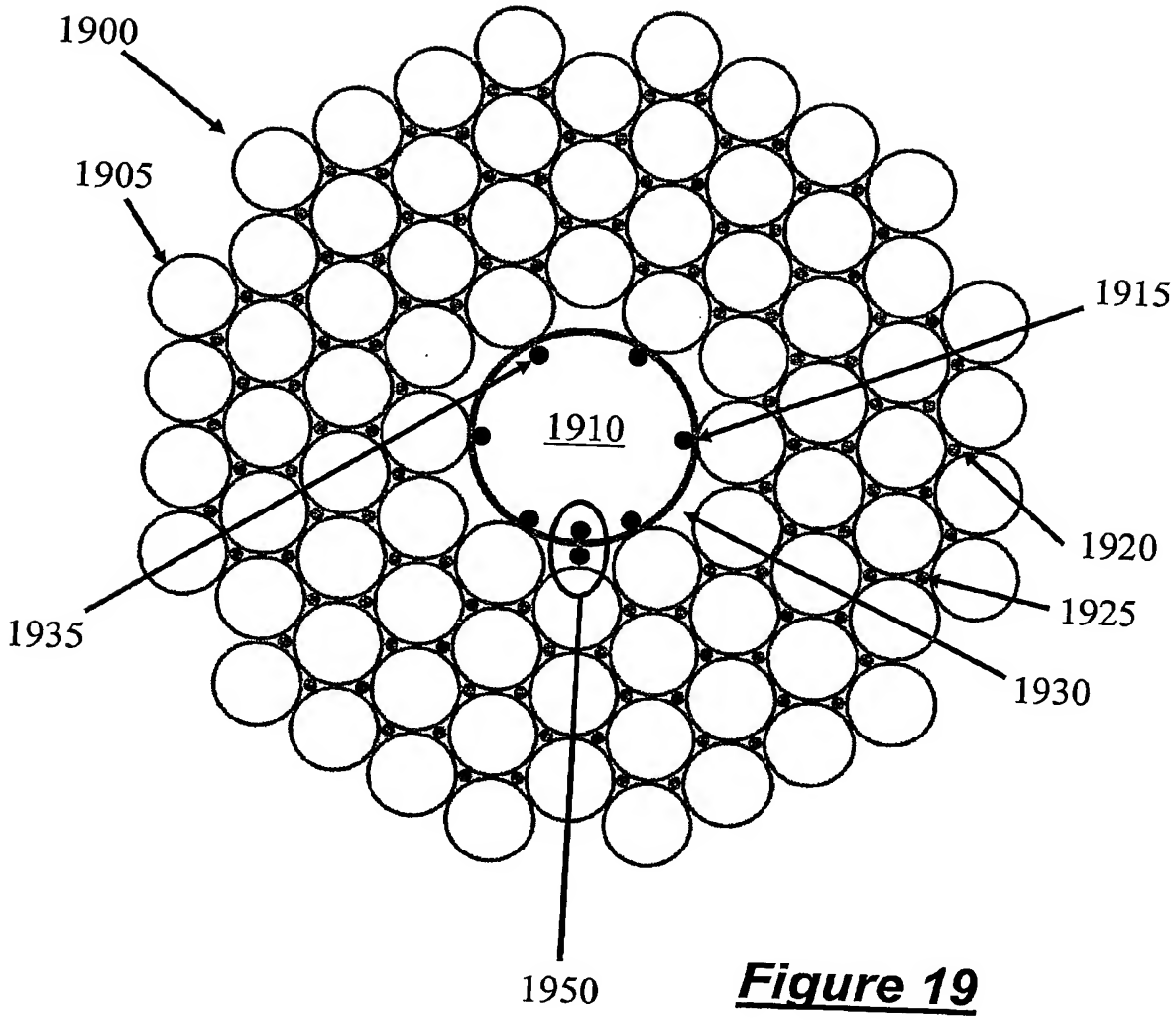

Figure 19

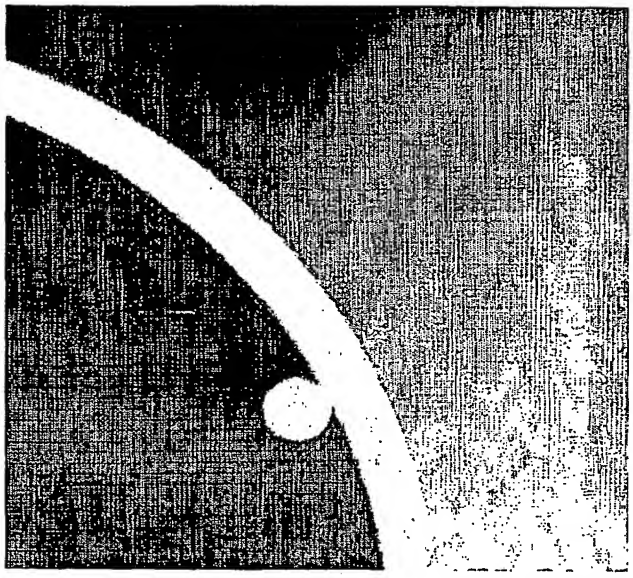

Figure 20a

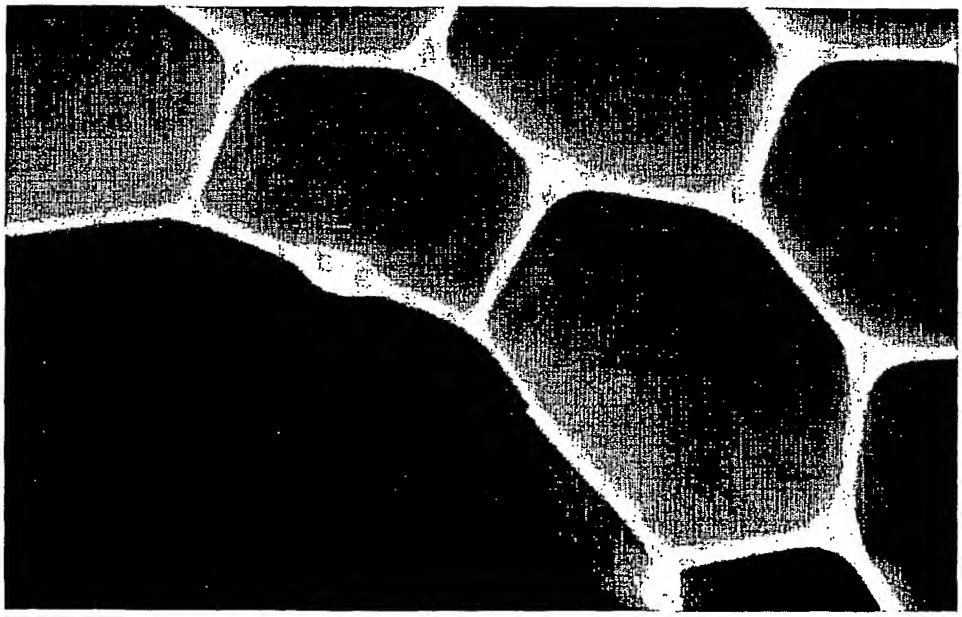

Figure 20b

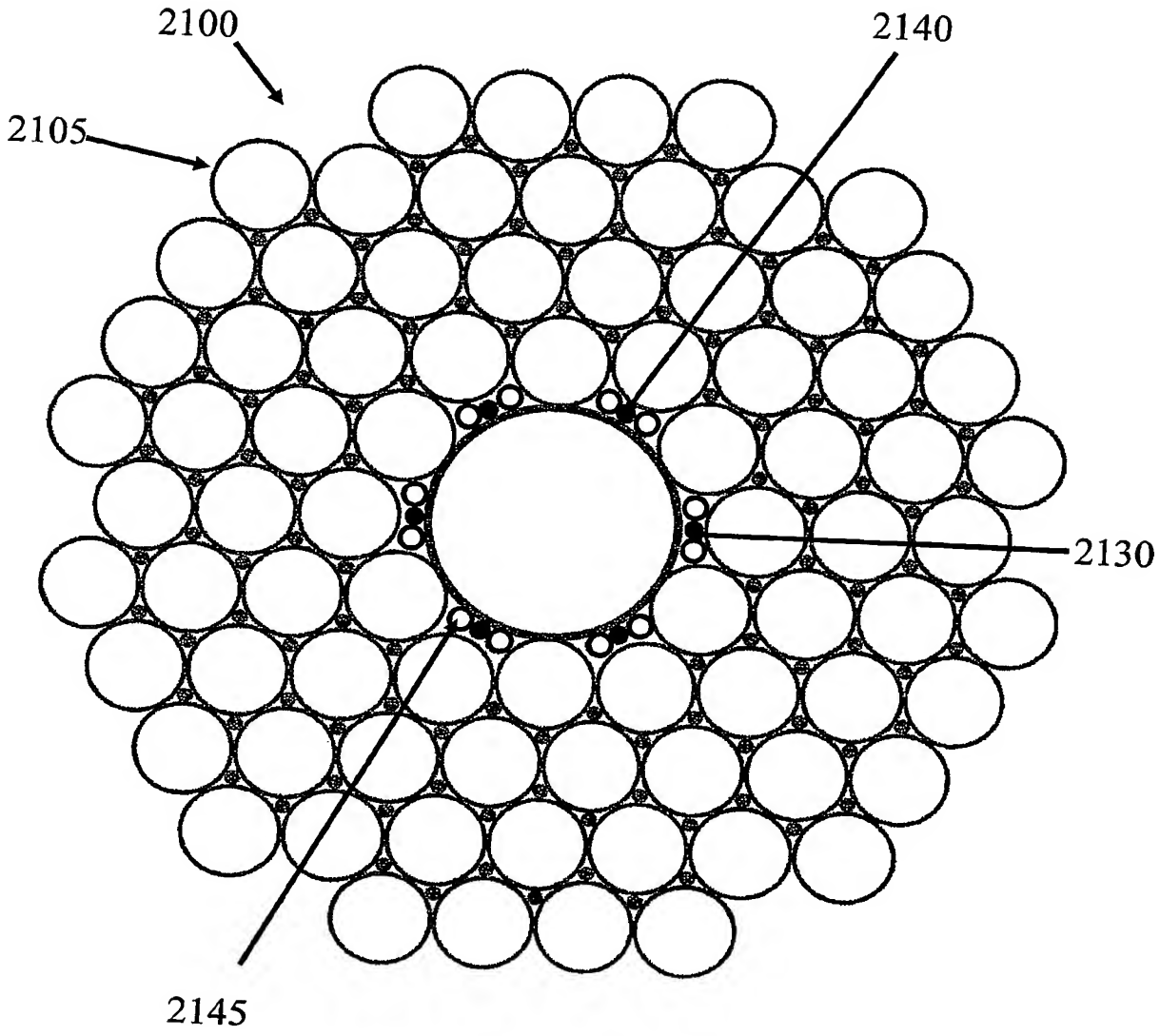

Figure 21

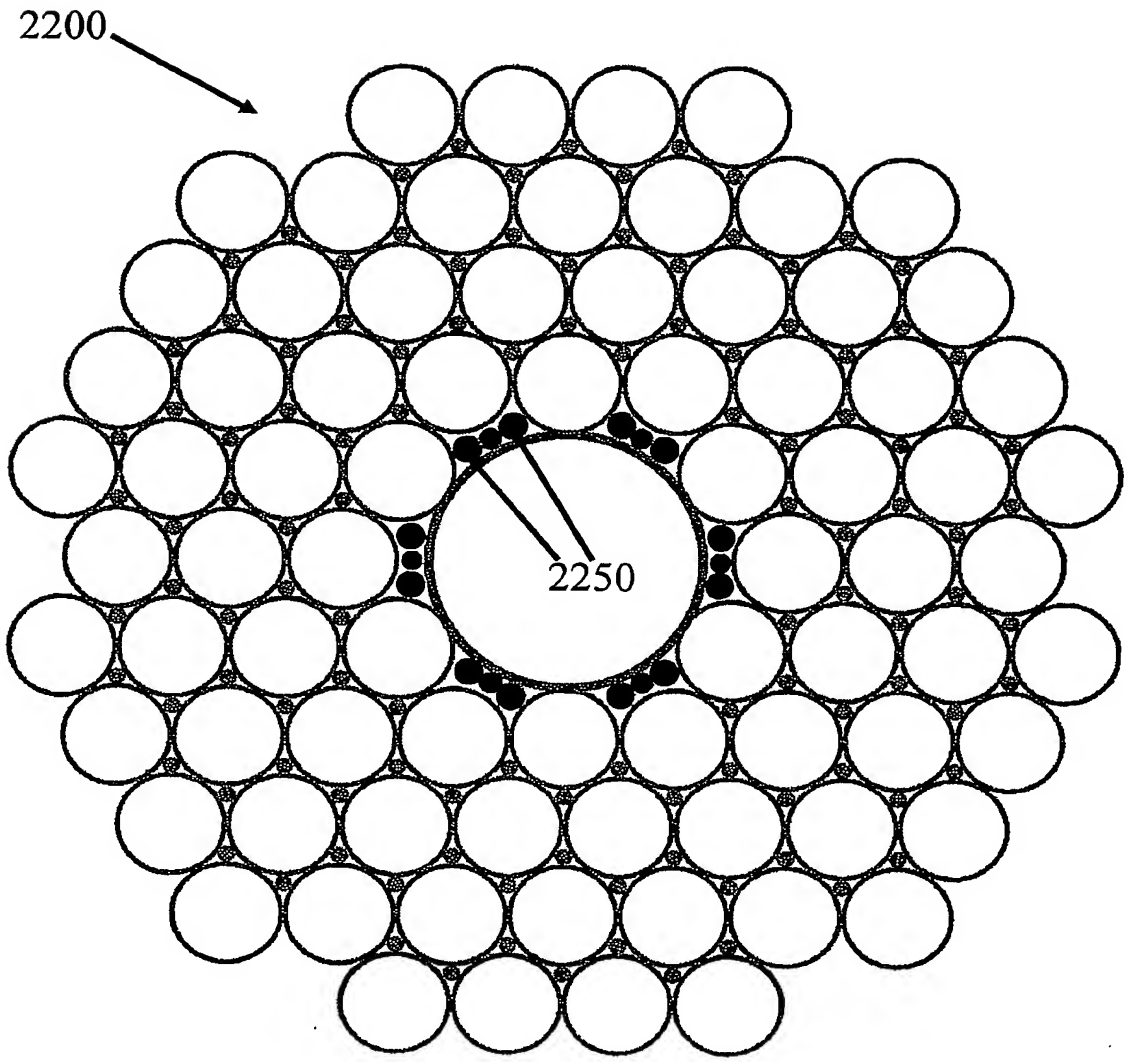

Figure 22

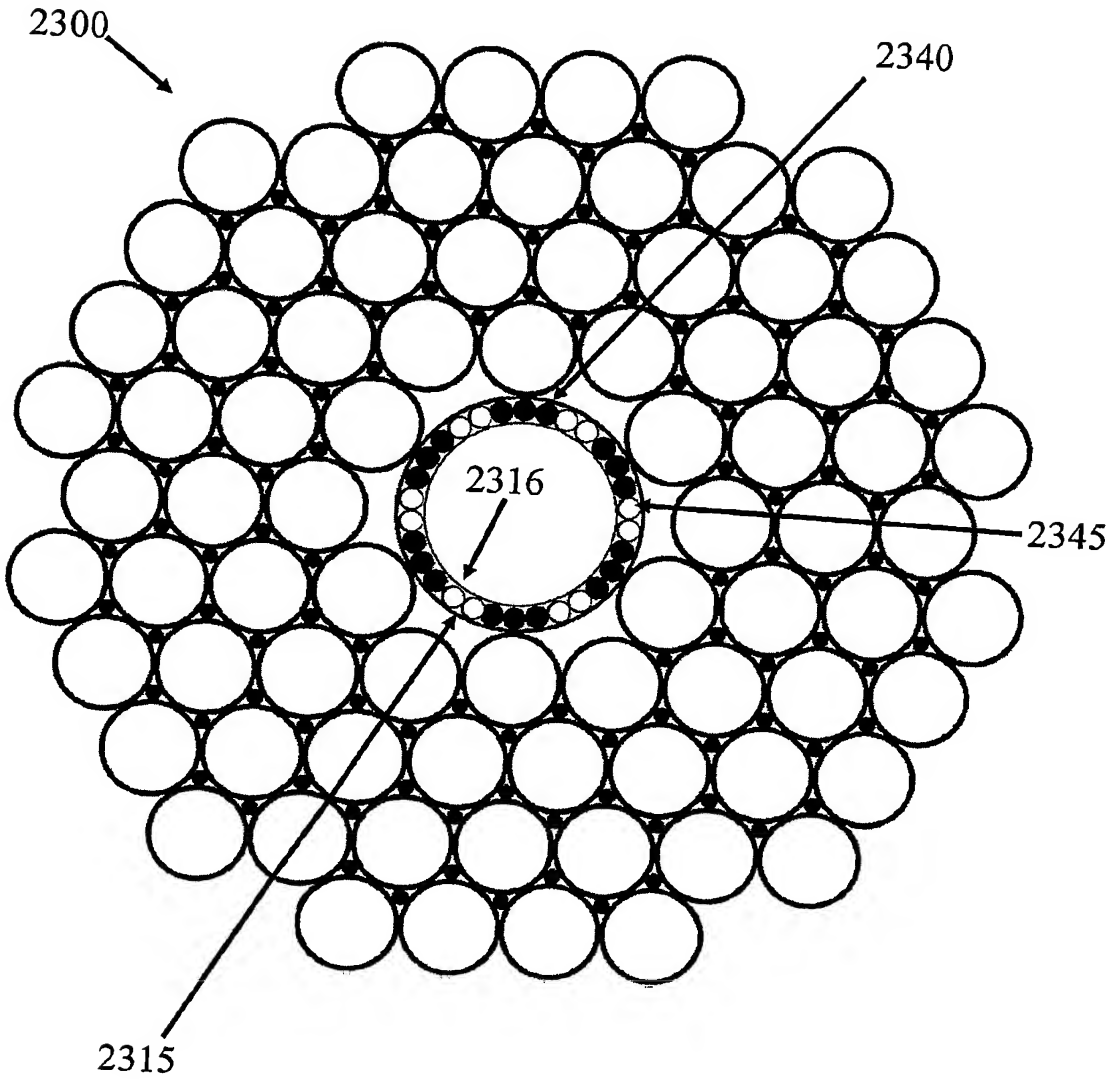

Figure 23

Figure 24a

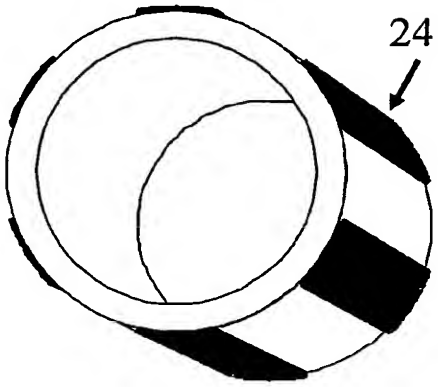

Figure 24b

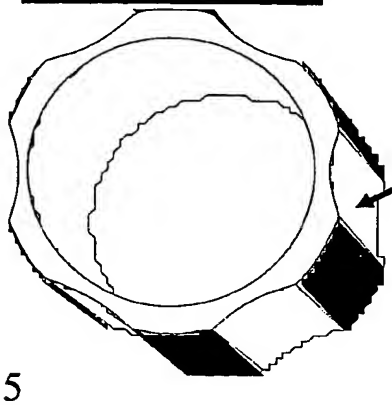

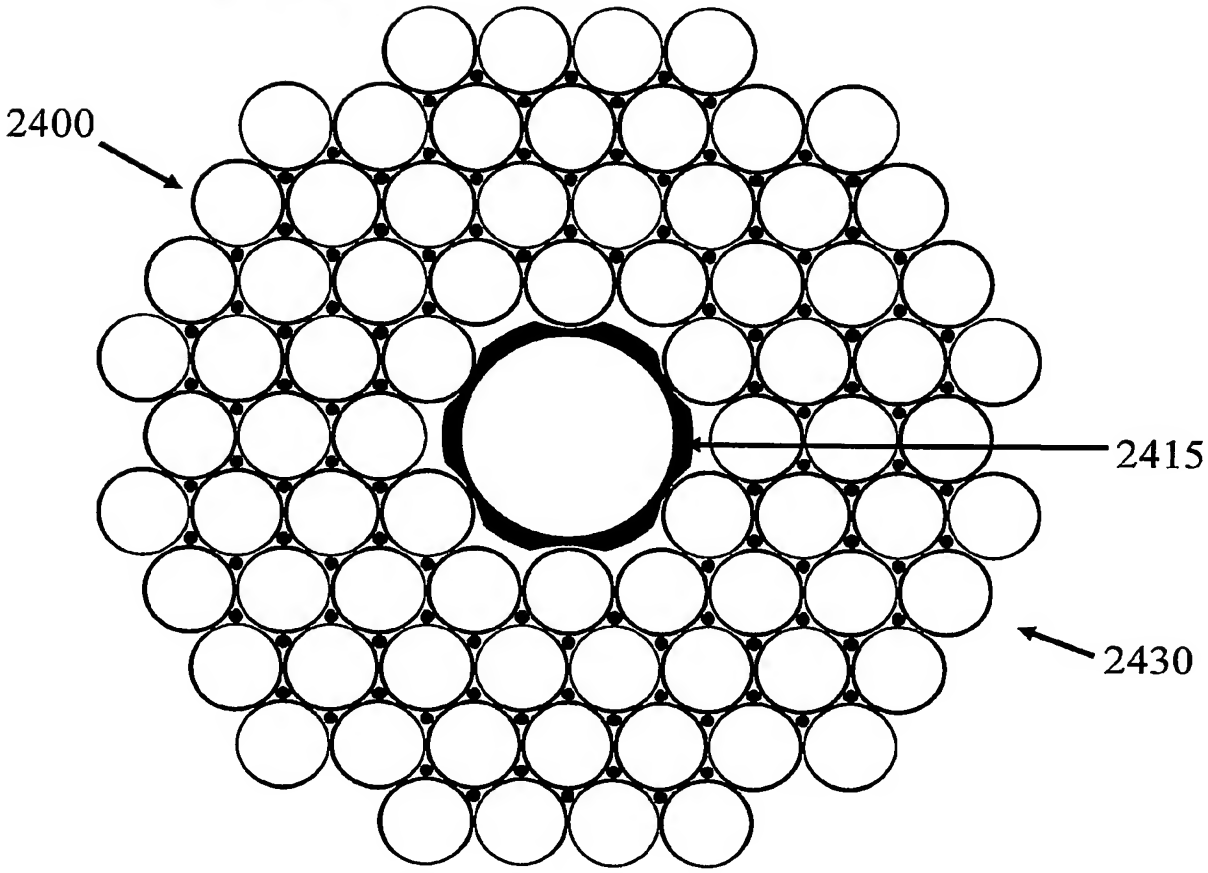

Figure 24c

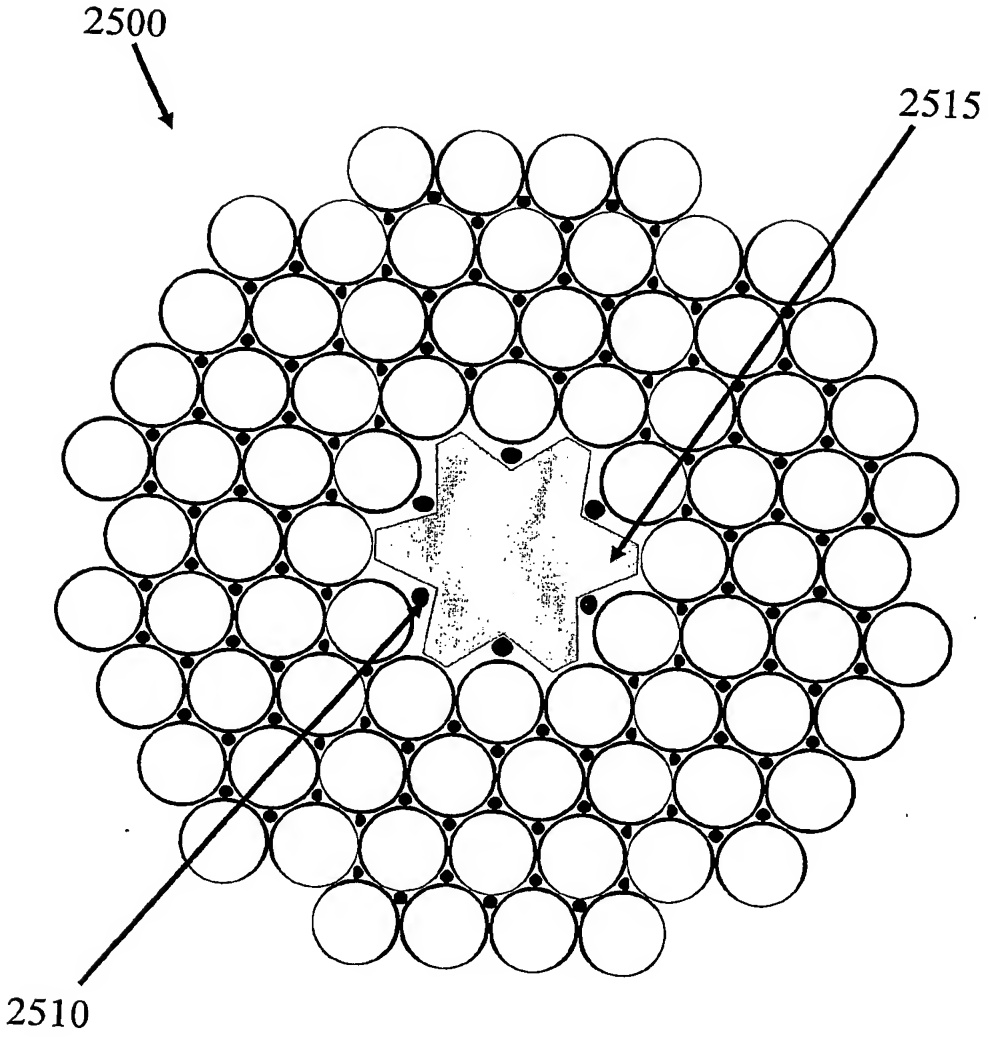

Figure 25

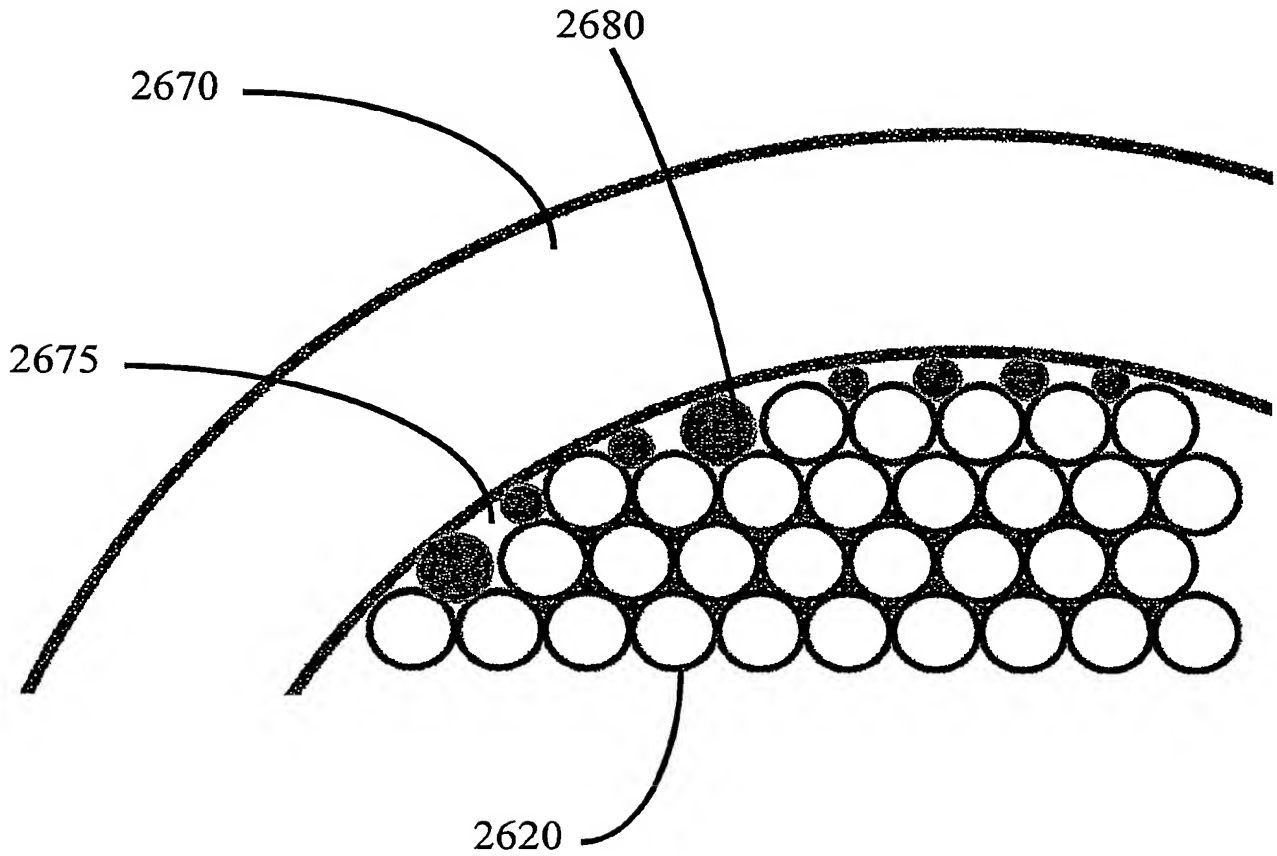

Figure 26

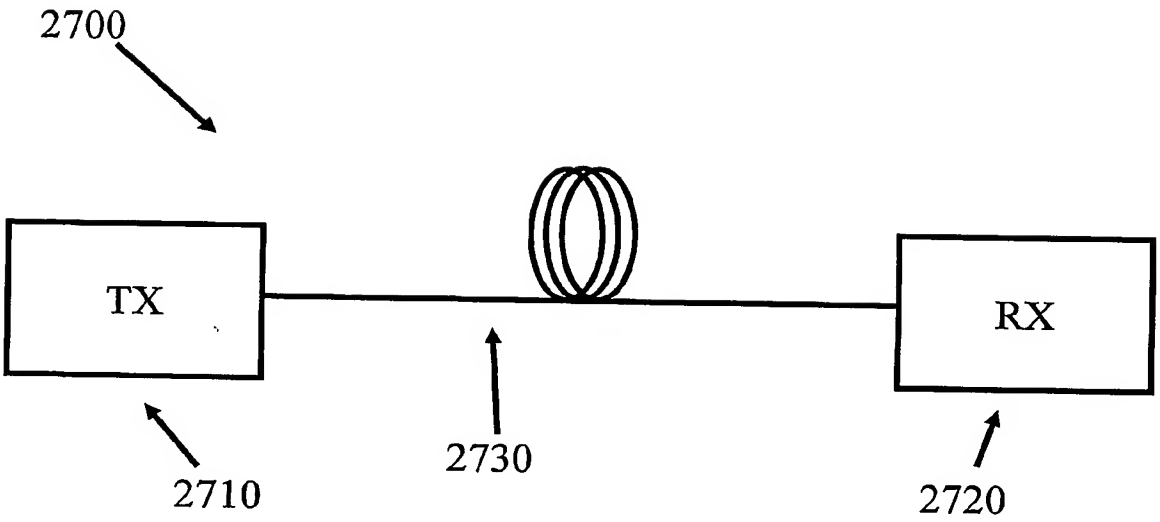

Figure 27

INTERNATIONAL SEARCH REPORT

Inter al Application No
PCT/GB 03/05591

A. CLASSIFICATION OF SUBJECT MATTER
IPC 7 G02B6/16 G02B6/20 C03B37/012

According to International Patent Classification (IPC) or to both national classification and IPC

B. FIELDS SEARCHED

Minimum documentation searched (classification system followed by classification symbols)
IPC 7 G02B C03B

Documentation searched other than minimum documentation to the extent that such documents are included in the fields searched

Electronic data base consulted during the international search (name of data base and, where practical, search terms used)
EPO-Internal, INSPEC, COMPENDEX

C. DOCUMENTS CONSIDERED TO BE RELEVANT

Category °	Citation of document, with indication, where appropriate, of the relevant passages	Relevant to claim No.
X	WO 99/64903 A (BARKOU STIG EIGIL ;BJARKLEV ANDERS OVERGAARD (DK); BROENG JES (DK)) 16 December 1999 (1999-12-16) page 9, line 4 - line 14; figure 8 page 12, line 25 page 16, line 11 -page 17, line 27 page 17, line 8 - line 20 page 22, line 27 -page 25, line 28 page 38, line 20 -page 39, line 25; figures 10-13,17-19 page 43, line 22 - line 28	1-45,47, 55-64

-/--

[X] Further documents are listed in the continuation of box C.

[X] Patent family members are listed in annex.

° Special categories of cited documents :

"A" document defining the general state of the art which is not considered to be of particular relevance

"E" earlier document but published on or after the international filing date

"L" document which may throw doubts on priority claim(s) or which is cited to establish the publication date of another citation or other special reason (as specified)

"O" document referring to an oral disclosure, use, exhibition or other means

"P" document published prior to the international filing date but later than the priority date claimed

"T" later document published after the international filing date or priority date and not in conflict with the application but cited to understand the principle or theory underlying the invention

"X" document of particular relevance; the claimed invention cannot be considered novel or cannot be considered to involve an inventive step when the document is taken alone

"Y" document of particular relevance; the claimed invention cannot be considered to involve an inventive step when the document is combined with one or more other such documents, such combination being obvious to a person skilled in the art.

"&" document member of the same patent family

Date of the actual completion of the international search	Date of mailing of the international search report
8 April 2004	23/04/2004

Name and mailing address of the ISA	Authorized officer
European Patent Office, P.B. 5818 Patentlaan 2 NL - 2280 HV Rijswijk Tel. (+31-70) 340-2040, Tx. 31 651 epo nl, Fax (+31-70) 340-3016	Bourhis, J-F

Form PCT/ISA/210 (second sheet) (January 2004)

INTERNATIONAL SEARCH REPORT

Interr l Application No
PCT/GB 03/05591

C.(Continuation) DOCUMENTS CONSIDERED TO BE RELEVANT

Category °	Citation of document, with indication, where appropriate, of the relevant passages	Relevant to claim No.
X	WO 02/072489 A (SKOVGAARD PETER M W ;BROENG JES (DK); CRYSTAL FIBRE AS (DK); JAKOB) 19 September 2002 (2002-09-19) page 11, line 20 -page 15, line 15; figures 4,5	1,2,4-6, 14, 17-26, 28, 42-48, 53-55
Y	KNIGHT J C ET AL: "PHOTONIC BAND GAP GUIDANCE IN OPTICAL FIBERS" SCIENCE, AMERICAN ASSOCIATION FOR THE ADVANCEMENT OF SCIENCE,, US, vol. 282, no. 5393, 20 November 1998 (1998-11-20), pages 1476-1478, XP001009986 ISSN: 0036-8075 page 1476 -page 1478	1-45, 55-64
Y	WO 02/075392 A (CORNING INC) 26 September 2002 (2002-09-26) cited in the application page 6, line 25 - line 28 page 10, line 30 -page 12, line 19; figures 7-10	1-45, 55-64
A	VENKATARAMAN N ET AL: "LOW LOSS (13 dB/km) AIR CORE PHOTONIC BAND-GAP FIBRE" ECOC 2002. 28TH. EUROPEAN CONFERENCE ON OPTICAL COMMUNICATION. POST-DEADLINE PAPERS. COPENHAGEN, DENMARK, SEPT. 8 - 12, 2002, EUROPEAN CONFERENCE ON OPTICAL COMMUNICATION.(ECOC), vol. CONF. 28, 12 September 2002 (2002-09-12), page PD11 XP001158363 cited in the application page PD11	1-44
A	DE 44 11 330 A (KUMACHOV MURADIN ABUBEKIROVIC ;VARTANJANC ALEKSANDR ZOLAKOVIC (RU)) 28 September 1995 (1995-09-28) column 6, line 54 - line 58 column 17, line 20 - line 55	49-52

INTERNATIONAL SEARCH REPORT

Ir tional application No.
PCT/GB 03/05591

Box I Observations where certain claims were found unsearchable (Continuation of item 1 of first sheet)

This International Search Report has not been established in respect of certain claims under Article 17(2)(a) for the following reasons:

1. ☐ Claims Nos.:
because they relate to subject matter not required to be searched by this Authority, namely:

2. ☒ Claims Nos.: 1-64
because they relate to parts of the International Application that do not comply with the prescribed requirements to such an extent that no meaningful International Search can be carried out, specifically:
see FURTHER INFORMATION sheet PCT/ISA/210

3. ☐ Claims Nos.:
because they are dependent claims and are not drafted in accordance with the second and third sentences of Rule 6.4(a).

Box II Observations where unity of invention is lacking (Continuation of item 2 of first sheet)

This International Searching Authority found multiple inventions in this international application, as follows:

1. ☐ As all required additional search fees were timely paid by the applicant, this International Search Report covers all searchable claims.

2. ☐ As all searchable claims could be searched without effort justifying an additional fee, this Authority did not invite payment of any additional fee.

3. ☐ As only some of the required additional search fees were timely paid by the applicant, this International Search Report covers only those claims for which fees were paid, specifically claims Nos.:

4. ☐ No required additional search fees were timely paid by the applicant. Consequently, this International Search Report is restricted to the invention first mentioned in the claims; it is covered by claims Nos.:

Remark on Protest

☐ The additional search fees were accompanied by the applicant's protest.

☐ No protest accompanied the payment of additional search fees.

Continuation of Box I.2

Claims Nos.: 1-64

Due to the use of vague terms and expresssion such as "enlarged region" and "around the boundary", present claims 1-64 relate to an extremely large number of possible products for which there is neither support of the claims in the description nor sufficient disclosure in the description for such an elongate waveguide and a preform.

In the present case, the claims so lack support, and the application so lacks disclosure, that a meaningful search over the whole of the claimed scope is impossible. Consequently, the search has been carried out for those parts of the claims which appear to be supported and disclosed, namely those parts relating to the fiber described on page 31, lines (18-28) in figure 16(a-d) of the present application (the ones shown on figures 15(a-d) are excluded by claim 1) and the methods described from page 32, line 23 to page 37, line 12.

The applicant's attention is drawn to the fact that claims, or parts of claims, relating to inventions in respect of which no international search report has been established need not be the subject of an international preliminary examination (Rule 66.1(e) PCT). The applicant is advised that the EPO policy when acting as an International Preliminary Examining Authority is normally not to carry out a preliminary examination on matter which has not been searched. This is the case irrespective of whether or not the claims are amended following receipt of the search report or during any Chapter II procedure.

INTERNATIONAL SEARCH REPORT

Intern Application No
PCT/GB 03/05591

Patent document cited in search report		Publication date	Patent family member(s)		Publication date
WO 9964903	A	16-12-1999	AU	755223 B2	05-12-2002
			AU	3026099 A	30-12-1999
			AU	755547 B2	12-12-2002
			AU	3810699 A	30-12-1999
			CA	2334510 A1	16-12-1999
			CA	2334554 A1	16-12-1999
			WO	9964904 A1	16-12-1999
			WO	9964903 A1	16-12-1999
			EP	1086393 A1	28-03-2001
			EP	1086391 A1	28-03-2001
			JP	2002517793 T	18-06-2002
			JP	2002517794 T	18-06-2002
			NZ	509201 A	26-11-2002
			US	6539155 B1	25-03-2003
WO 02072489	A	19-09-2002	WO	02072489 A2	19-09-2002
WO 02075392	A	26-09-2002	EP	1370893 A2	17-12-2003
			TW	539875 B	01-07-2003
			WO	02075392 A2	26-09-2002
			US	2002136516 A1	26-09-2002
DE 4411330	A	28-09-1995	DE	4411330 A1	28-09-1995

THIS PAGE BLANK (USPTO)